

書式変更: 単語の途中で改行する

Measurement of ~~micro~~tiny-droplets using a newly developed optical fibre probe microfabricated by femtosecond pulse laser

書式変更: 間隔 段落前 : 0 pt, 段落後 : 0 pt

T. Saito¹, K. Matsuda^{1,2}, ~~T. Saito~~², Y. Ozawa^{1,2}, S. Oishi³, S. Aoshima³

書式変更: フォント : Times, 11 pt

書式変更: Authors、行間 : 1 行

¹ Corresponding author, Shizuoka University, 3-5-1 Johoku, Naka-ku Hamamatsu, Shizuoka 432-8561, Japan. E-mail: ttsaito@ipc.shizuoka.ac.jp
~~Shizuoka University, 3-5-1 Johoku, Naka-ku Hamamatsu, Shizuoka 432-8561, Japan~~

書式変更: フォント : 太字 (なし)

² Shizuoka University, 3-5-1 Johoku, Naka-ku Hamamatsu, Shizuoka 432-8561, Japan Corresponding author, Shizuoka University, 3-5-1 Johoku, Naka-ku Hamamatsu, Shizuoka 432-8561, Japan. E-mail: ttsaito@ipc.shizuoka.ac.jp

書式変更: フォント : 太字 (なし)

³ CRL, Hamamatsu Photonics K.K., 5000 Hirakuchi, Hamakita-ku Hamamatsu, Shizuoka, 434-8601

Abstract. Optical fibre probing is widely applied to measurement in gas-liquid two-phase flows. We already developed and reported a Four-Tip Optical fibre Probe (F-TOP) for millimetre-size bubbles/droplets, and a Single-Tip Optical fibre Probe (S-TOP equipped with a wedge-shaped tip) for sub-millimetre-size bubbles/droplets. However, it is difficult to measure micrometre-size bubbles/droplets by S-TOP. The main purpose of the present study was to develop a new type of optical fibre probe micro-fabricated by a femtosecond pulse laser (~~fs-ProbeFs-TOP~~). First, we confirmed the performance of the new probe by examining millimetre- and sub-millimetre-size droplets; the results by ~~fs-ProbeFs-TOP~~ were compared with those obtained from the visualization of the droplets by high-speed video camera, and showed satisfactory agreement. In addition, we demonstrated the measurement of velocities and chord lengths of micrometre-size droplets (about 50 µm in diameter) using the ~~fs-ProbeFs-~~

書式変更: 両端揃え

Matsuda & Saito_MST/307768

書式変更: 単語の途中で改行する

TOP
Listed in the
reference list.
for Q1

... with those by S-TOP to clarify the limits and
streng... probe.

Keywords: Optical fibre probe, femtosecond pulse laser, droplet, chord length, velocity,
simultaneous measuremen

Revised.
for Q2 and Q9

1. INTRODUCTION

Gas-liquid two-phase flows are frequently encountered in a wide range of industrial fields. Recently, demands for measurement of tiny bubbles/droplets have emerged in the a variety of research fields of, e.g., sprays, automotive engines, fine chemistry, and atomic power plants, and so on. A highly-accuracy measurement method for characterization of bubbles/droplets at high number-density has been yearned for in laboratory and industrial use. Various methods for the such measurement have been proposed, however, it is very difficult to find a real-time and high-accuracy measurement method to satisfy industrial needs has even difficult. An optical fibre probes is can be applied to the measurement of gas-liquid two-phase flows (e.g. Abuaf et al 1978). Much research into this method has been conducted. For millimetre-size bubbles/droplets (i.e., larger than 4 mm in equivalent diameter, after mm-size bubble/droplet), a multi-tip optical fibre probe is very useful (e.g. Mudde & Saito 2001; Saito et al 2001, 2004). The influences of the piercinged positions on measurement chord lengths were has been studied in consideration with regard to statistical factors (Calk et al., 1988, 1995). However, simultaneous measurement of their chord lengths and velocities has been thought to need-require at least two optical fibre probes due to the probes' measurement principle. On the other hand, Catellier et al. (1990, 1991, 1992, 1998), and Higuchi et al (2004) have been studying the simultaneous measurement of velocities, chord lengths and void fractions of bubbles/droplets via-by a multi-fibre optical probe.

Recently, particular demands for measuring the properties of micro droplets/bubbles have increased in research in multi-phase flow researchs. For the measurements of tiny droplets/

書式変更: 両端揃え

書式変更

書式変更

コメント [KN1]: ?"the probes"?"

書式変更: フォント : Times New Roman

書式変更: フォント : 斜体

書式変更: フォントの色 : 赤

書式変更

書式変更

書式変更

書式変更

書式変更

bubbles ~~via by~~ optical fibre probe, a multi-tip probe is not applicable, because the multi-tip optical fibre probe is too large to ~~surely pierce~~ ~~such spheresthem~~. In order to solve this problem, the authors developed a Single-Tip Optical-fibre Probe (S-TOP) which realizes the simultaneous measurement of chord lengths and velocities of tiny bubbles/droplets at low velocities (Saito 1999, 2002). However, ~~it this probe is difficult to cannot~~ measure micro droplets/bubbles at high velocities ~~by the S-TOP owing to because of~~ its measurement principle. To ~~break through overcome~~ this problem, we have developed a new type of optical fibre probe micro-fabricated by femtosecond pulse laser (~~fs-ProbeFs-TOP~~), which realizes simultaneous measurement of chord lengths and velocities of tiny droplets/bubbles at high velocities.

The S-TOP and ~~fs-ProbeFs-TOP~~ ~~have the distinguished properties compared with the other former probes.~~ Each optical probe ~~has have~~ different kinds of characteristics; therefore, they should be ~~used underselected with~~ careful consideration of ~~their~~ application ranges ~~reflecting their characteristics~~. In the present paper, those characteristics ~~and the comparisons of them~~ are described ~~and compared. B~~ based on the ~~comparisons between correlation of the~~ measurement results ~~of each of the S-TOP/fs-Probe and with~~ those of visualization, ~~we consider their characteristics and compare their performance as follows.~~

~~In addition, we propose various methods for interpreting the results. In~~ a single probe method, the probe should pierce the centre region of a droplet/bubble in order to accurately measure its minor axis. ~~First, we propose a~~ Our newly developed method ~~using a pre-signal to can~~ detect whether the S-TOP/~~fs-ProbeFs-TOP~~ ~~has pierces~~ the centre region of a droplet/bubble. ~~Second, w~~ We also discuss the forced deformation when the probe touches the droplet interface. ~~Focusing on, and its relation to~~ droplet's size and velocity, ~~we discuss this deformation.~~ ~~Third, w~~ We carefully discuss ~~the influences of the droplet another~~ deformation ~~taking place of the droplet during the S-TOP/fs-Probe measurement (i.e.; namely, that~~ while the probe is piercing ~~the droplet on the measurement results~~). Based on these ~~theoretical~~ discussions, we ~~describe interpret~~ the actual results of ~~millimetre-size and sub-millimetre-size~~ (300 □ 600 μm, sub-mm-size) droplet ~~droplet~~ measurements ~~via by~~ S-TOP and ~~fs-ProbeFs-TOP~~. We confirm the performance and properties of the S-TOP/fs-Probe by examining ~~millimetre droplets, sub millimetre size droplet (sub mm size droplet).~~ In addition, we

コメント [KN2]: This was a generalization that was not supported by any details of the paragraph, so I deleted it.

書式変更

... [1]

書式変更: フォント : Times New Roman

書式変更: 両端揃え

書式変更

... [2]

コメント [KN3]: This language is rather vague. How does this differ from the deformation at the interface?

書式変更

... [3]

Matsuda & Saito_MST/307768

書式変更: 単語の途中で改行する

demonstrate the measurement of velocities and chord lengths of millimetre-size (50 □ 100 μm in equivalent diameter, μm-size) droplets using the fs-ProbeFs-T

書式変更

書式変更: フォント: Times New Roman

Revised for Q3

2. EXPERIMENTS

2.1 Single-Tip Optical fibre Probe (S-TOP) and new type of optical fibre probe (fs-ProbeFs-TOP) [You need "steel" after "stainless" below.]

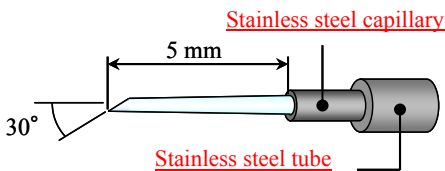


Figure 1. Structure of S-TOP.

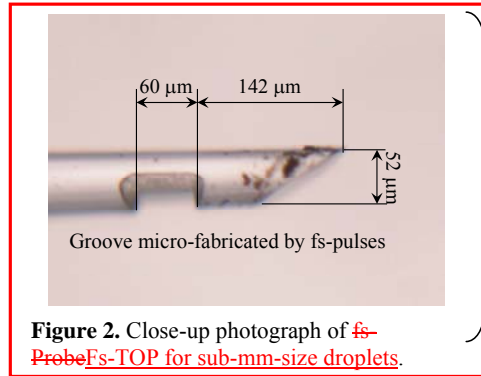


Figure 2. Close-up photograph of fs-ProbeFs-TOP for sub-mm-size droplets.

Answer-R3-3

書式変更: フォント: Times New Roman, 太字, フォントの色: ピンク

書式変更: フォント: Times New Roman, 太字, フォントの色: ピンク

2.1.1 S-TOP. Figure 1 shows the structure of the S-TOP used in the present study. The S-TOP was made of a synthetic silica optical fibre (external diameter, 230μm; core diameter, in external diameter, 190μm in core diameter; jacket thickness, 15μm; refractive index in jacket thickness, 1.46 in refractive index). The silica optical fibre was fine-drawn using a micropipette puller (P-2000, Sutter Instrument Company). After that, the tip was ground in at an angle of 30 degrees with to the fibre axis via by a micropipette beveller (BV-10, Sutter Instrument Company); the most distinguishable feature of the S-TOP is that its tip is ground

書式変更: 両端揃え

~~in at~~ an angle of 30 degrees ~~with to~~ the fibre axis. The tip diameter is 20 μ m. This fibre was inserted and fixed in a stainless capillary. Accordingly, chord lengths and velocities of bubbles/droplets are measured using only a single-tip optical fibre probe. Furthermore, S-TOP is coated with ~~a~~ water repellent material by vacuum evaporation ~~of a water repellent material~~ in order to control the surface wettability.

2.1.2 ~~fs-ProbeFs-TOP~~. Figure 2 shows the structure of the ~~fs-ProbeFs-TOP~~ used in the present study. The ~~fs-ProbeFs-TOP~~ was made of a synthetic silica optical fibre (~~external diameter~~, 230 μ m; ~~core diameter in external diameter~~, 190 μ m; ~~jacket thickness in core diameter~~, 15 μ m; ~~refractive index in jacket thickness~~, 1.46 ~~in refractive index~~). The silica optical fibre was also fine-drawn using the micropipette puller. After that, the clad near the tip was processed by femtosecond pulses. A close-up picture is shown in ~~Figure~~ 2. Since a clad is stripped from a core at the groove, the core touches ~~the~~ air directly. The phase detection is done in two stages (i.e. at tip of the probe and at the groove). This fibre was inserted and fixed in a stainless capillary. ~~Furthermore, the fs-ProbeFs-TOP is also~~ coated with water repellent material by vacuum evaporation ~~of a water repellent material~~.

2.2 Rational targets for S-TOP and ~~fs-ProbeFs-TOP~~ measurements.

The S-TOP and ~~fs-ProbeFs-TOP~~ have the ~~distinguished distinguishing~~ properties compared with ~~the other~~ conventional probes. Furthermore, our probes have different characteristics owing to ~~the differences in their of~~ measurement principles and manufacturing processes. The S-TOP can be made very easily; the tip of the S-TOP is only micro-ground into a wedge shape. Hence, the wedge-shaped tip is gradually covered with the ~~other opposite~~ phase (liquid phase in the cases of ~~the~~ droplet measurement; ~~the~~ gas phase in the cases of ~~the~~ bubble measurement). ~~By contrast, m~~Micro-fabrication of ~~the fs-ProbeFs-TOP~~ ~~needs requires~~ a high-power femtosecond-pulse laser, nano-order 6-axes automatic optical stages, confocal optics, and so on. ~~The fabrication~~It is very difficult to ~~make fabricate~~ the ~~fs-ProbeFs-TOP~~ with ~~the~~ desired performance.

It is important to use intelligently ~~both select between these two probes~~ ~~due according~~ to the measurement objective, based on ~~a thorough~~ understanding of their properties.

書式変更: 両端揃え

コメント [KN4]: You do not support this statement with details.

書式変更: 両端揃え, 1 行の文字数を指定時に右のインデント幅を自動調整しない, 改ページ時 1 行残して段落を区切る, 句読点のぶら下げを行わない, 日本語と英字の間隔を自動調整しない, 日本語と数字の間隔を自動調整しない, グリッドへ配置しない

Figure 3 shows ~~the a~~ schematic diagram of ~~the~~ measurement processes ~~by~~ using the S-TOP and ~~fs-ProbeFs-TOP~~. The S-TOP measures the velocities of bubbles/droplets by ~~a~~ very small tip. Hence, the S-TOP needs ~~the a~~ fast A/D converter and fast amplifier for the measurements of tiny bubbles/droplets moving at high velocity. This is a disadvantage of S-TOP measurement. Therefore, the measurement object of the S-TOP is the sub-mm-size droplet moving ~~at~~ less than several m/s.

On the other hand, the measurement object of ~~the fs-ProbeFs-TOP~~ is ~~the um-size -micro-~~ droplets and sub-mm-size droplets moving at ~~over~~ 10 m/s or more. The ~~fs-probeFs-TOP~~ uses the signal from the probe tip and that from the groove. Hence, the time interval of the event time becomes larger than that of ~~the~~ S-TOP.

The S-TOP and ~~fs-ProbeFs-TOP~~ have ~~the~~ different application ranges, respectively. In this paper, we confirm the performance of the ~~fs-ProbeFs-TOP~~ and S-TOP by examining millimetre- and sub-mm-size droplets for the first time. When the droplet velocity is around 10 m/s, the ~~fs-ProbeFs-TOP~~ can ~~highly accurately~~ measure the droplet property ~~with higher accuracy compared with~~ ~~than~~ the S-TOP.

2.3 Optics and data acquisition.

The optics ~~system~~ is shown in ~~Fig-figure~~ 4. The beam from a laser diode (a) (wavelength 635nm) is split by ~~a~~ beamsplitter (b), and focused on the fibre edge (d) by ~~an~~ objective lens (c). ~~A p~~ Part of the laser beam propagated through the optical fibre is reflected at the other tip (sensing side) of the optical fibre probe, changed its own polarization plane at the reflection and propagated back again through the same fibre; then it is input into a photo multiplier (f) through a polarizer (e) cutting the laser beam (i.e. the beam from the laser diode) with a different polarization plane from that of the reflected beam. ~~Part of the laser beam propagated through the optical fibre is reflected at the other tip (sensing side) of the optical fibre probe, and propagated back again through the same fibre; then it was is input into a photo-multiplier (f) through a polarizer (e) cutting a direct laser beam from the laser diode.~~

The optical signal was converted into an electrical signal ~~vi~~ ~~aby~~ ~~the~~ photo multiplier (f). The electrical signal was stored in ~~a~~ digital oscilloscope (g) (sampling rate 200 MHz).

2.3 Experimental setups.

Figure 5 shows a schematic diagram of the experimental setup used in demonstration of millimetre-size droplet (droplet diameter: $1 \text{ mm} < L_D \leq 5 \text{ mm}$;) measurement by Fs-TOP and S-TOP. Droplets are launched from a micro capillary (h) ($780 \text{ }\mu\text{m}$ in inner diameter) placed over the probe (a). The equivalent diameter of the droplets is 2 mm , and their velocities varied between 0.25 m/s and 2.5 m/s . We visualized the process of the droplets being pierced by the S-TOP using a high-speed video camera (e) (frame rate, 2900 fps ; exposure time, $50 \text{ }\mu\text{s}$; resolution, $800 \times 512 \text{ pixel}^2$; and spatial resolution, $21.97 \text{ }\mu\text{m}/\text{pixel}$) and a halogen light (g).

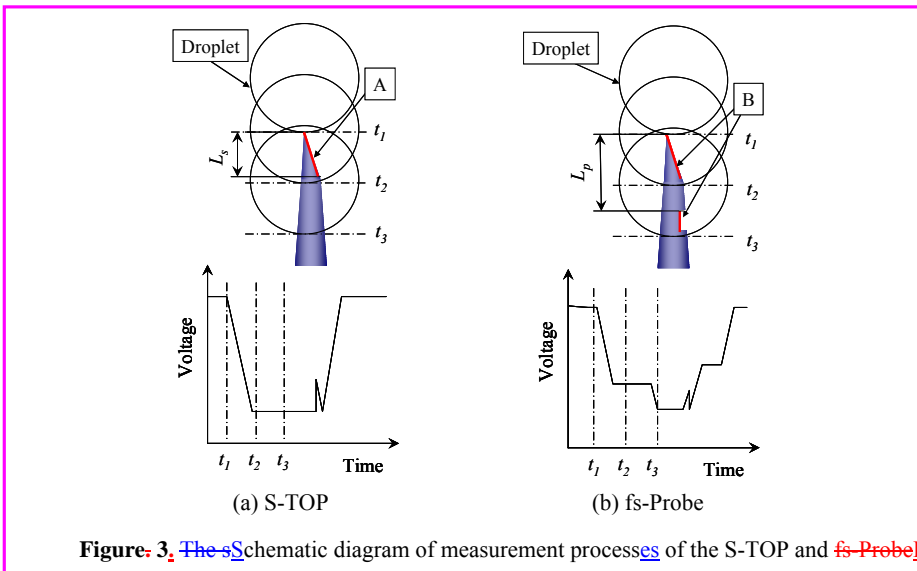


Figure 3. The schematic diagram of measurement processes of the S-TOP and fs-Probe.

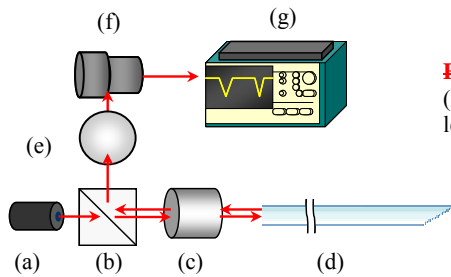


Figure 4. Optics.

(a) Laser diode, (b) Beamsplitter, (c) Objective lens, (d) Optical fibre probe, (e) Polarizer,

Figure 4. Optics.

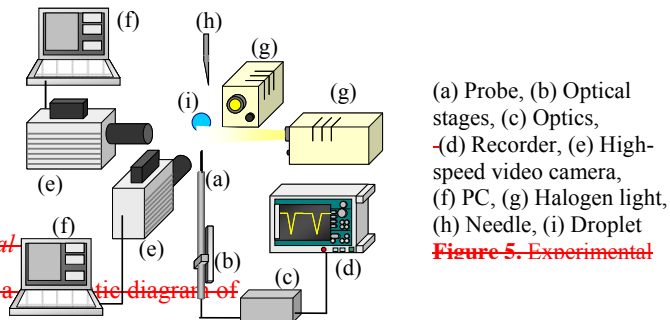


Figure 5. Experimental

2.3 Experimental

Figure 5 shows a schematic diagram of

the experimental setup used in the demonstration of millimetre-size droplets

(droplet diameter: $1 \text{ mm} \leq L_D \leq 5 \text{ mm}$;) measurement via by fs-Probe and S-TOP.

Droplets are launched from a micro

capillary (h) ($780 \mu\text{m}$ in inner diameter)

placed over the probe (a). The equivalent

diameter of the droplets is 2 mm, and their

velocities were varied between 0.25 m/s

and 2.5 m/s. We visualized the process of

the droplets being pierced with by the S-

TOP using a high-speed video camera (e)

(frame rate, 2900 fps, exposure time, 50

μs , resolution, $800 \times 512 \text{ pixel}^2$, and

spatial resolution, 21.97 $\mu\text{m}/\text{pixel}$) and a halogen light (g).

書式変更: 両端揃え

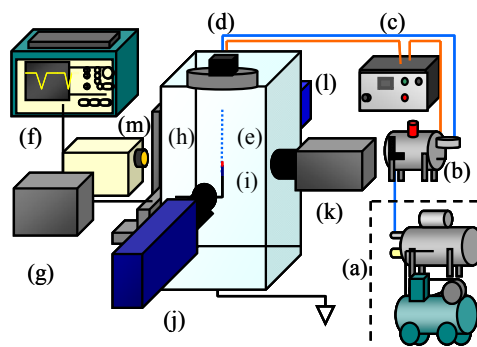
Figure 6 shows a schematic diagram of the experimental setup used in experiments of sub-mm-size droplets (droplet diameter: $150 \mu\text{m} \leq L_D \leq 500 \mu\text{m}$; droplet velocity: $5 \text{ m/s} \leq U_D \leq 25 \text{ m/s}$) measurement via ~~fs-ProbeFs-TOP~~ and S-TOP. Ion-exchange water in ~~the a~~ water tank (b) ~~is was~~ pressurized by air (a) (gauge pressure $25 \text{ kPa} \leq P \leq 300 \text{ kPa}$), and the pressurized water was ejected from ~~the~~ nozzle (nozzle diameter $D = 30, 60, 100, 150, 200 \mu\text{m}$) (e). ~~The~~ diameters of the droplets ~~is~~ varied between $150 \mu\text{m}$ and $500 \mu\text{m}$, and their velocity was varied between 5 m/s and 25 m/s . The probe was mounted on a three-degree-of-freedom precision micro stage (h) driven by micro stepping motors. The probe position was adjusted precisely using the micro stage, as the probe was able to strike the ~~μm -size-micro~~ droplets. The process of ~~the~~ piercing ~~of~~ droplets with the probe was also visualized using two high-speed video cameras (j) (frame rate 250000, 500000, 1000000 fps; exposure time, $0.5 \mu\text{s}$; resolution, $260 \times 312 \text{ pixels}^2$; and spatial resolution, $6.67 \mu\text{m}/\text{pixel}$) (k), and a strobe light (l) and a halogen light (m).

書式変更: フォントの色 : 黒

Figure 7 shows the schematic diagram of the experimental setup ~~which~~ used in ~~the~~ experiments of ~~μm -size-micro~~ droplets measurement ~~via by fs-ProbeFs-TOP~~. Micrometer-size droplets (droplet diameter: $L_D \approx 30 \mu\text{m}$, droplet velocity; $1.5 \text{ m/s} \leq U_D \leq 2.5 \text{ m/s}$) ~~is were~~ ejected from ~~the a~~ piezoelectric ink jet nozzle (h). We visualized the contact process between the droplets and the ~~fs-ProbeFs-TOP~~ by using a ~~H~~high-speed video camera (e) and a ~~s~~Strobe light (g).

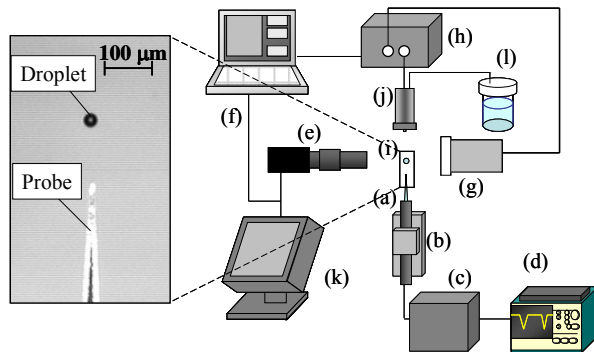
書式変更: フォントの色 : 黒

書式変更: フォントの色 : 黒



(a) Pressurization source, (b) Water tank, (c) Pressure controller, (d) Electromagnetic valve, (e) Piezo nozzle, (f) Digital oscilloscope, (g) Optical system, (h) 3-axis unit, (i) S-TOP, (j) High-speed video camera 1, (k) High-speed video camera 2, (l) Strobe light, (m) Halogen light source.

Figure 6. Experimental setup for measurement of sub-millimetre-size droplets.



(a) Probe, (b) Optical stages, (c) Optical system, (d) Digital oscilloscope,
 (e) High-speed video camera, (f) PC, (g) Strobe light, (h) Piezoelectric ink jet nozzle,
 (i) Droplet,
 (j) Controller, (k) Monitor, (l) Water tank

Figure 7. Experimental setup for measurement of μ micrometre-size droplets.

(a) Probe, (b) Optical stages, (c) Optical system, (d) Digital oscilloscope,
 (e) High speed video camera, (f) PC, (g) Strobe light, (h) Piezoelectric ink jet nozzle, (i)
 Droplet,
 (j) Controller, (k) Monitor, (l) Water tank

3. SIGNAL PROCESSING

3.1 Signal processing for S-TOP.

3.1.1 Characteristics of S-TOP signals. A typical signal in droplet measurements via by the S-TOP is plotted in figure Fig. 8. The wedge-shaped tip of the S-TOP is gradually covered with the other phase; in consequently ee the intensity of the light reflected at the tip is gradually changed (marked in figure Fig. 8); the interface velocity is proportional to the derivative of the optical signal (derivative of the leading edge of optical signal) with respect to time (Saito 2007 a, b). Therefore, measuring the surface tension and viscosity of measurement objects preliminarily, a the gas-liquid interface velocity is easily calculated by using this relation (e.g. Saito *et al.* 2000, Saito 2007 c). Accordingly, chord lengths and velocities of bubbles/droplets are were measured using only a single tip optical fibre probe. The gradient of a the leading edge g_{rd} is calculated by equation (1),

$$g_{rd} = \frac{dV}{dt} \times \frac{1}{(V_{Gas} - V_{Liquid})}, \quad (1)$$

where dV/dt is obtained from a burst signal, and the gas-phase output level V_{Gas} and liquid-phase level V_{Liquid} are calculated as described in section 3.1.2. In a similar way, the gradient of the rising edge is calculated by the equation (1).

The droplet velocity U_D (in a strict sense, the average interface velocity of a droplet) is calculated from equation (2)

$$U_D = \frac{1}{\alpha} \times g_{rd}, \quad (2)$$

where α is the proportionality coefficient between the interface velocity and g_{rd} . The coefficient “ α ” depends on only 3 factors as follows: the angle of the S-TOP tip, the wettability between the probe and the liquid phase, and the surface tension of the liquid phase. The angle of the S-TOP tip is decided based on the results of ray trace calculation considering the difference of in refraction indexes between the core of the optical fibre and the liquid phase. After that, the value of the coefficient “ α ” is decided by only the properties

of the liquid phase (the wettability and surface tension). In this paper, these properties do not change, because we measure only water droplets.

Figure 89 shows the relationship between g_{rd} obtained by S-TOP measurements and U_D by visualization. As shown in this figure, the value of the coefficient “ α ” of the calculated value 5.60×10^{-6} is adequate.

The chord length L_D is calculated from equation (3),

$$L_D = U_D \times (t_e - t_s), \quad (3)$$

変更されたフィールド コード

where t_s and t_e are the starting and finishing-end times of contact between the S-TOP and the droplet. The event time t_s is defined as an intersection point of the straight line (i.e. the gradient is g_{rd}) and the gas-phase level at the leading edge. The event time t_e is defined as the intersection point of the straight line (i.e. the gradient is g_e) and the liquid-phase level at the rising edge.

書式変更: 両端揃え

3.1.2 Evaluation of droplet deformation and Pre-signal. Figure 10 shows schematic drawings of the S-TOP/fs-Probe measurement. When the probe pierces the centre region of a droplet/bubble, the chord length obtained via probe is very similar to the droplet's/bubble's minor axis. In the measurements of droplets/bubbles, if L_M is limited within an area of $L_M / L_{Bl} < 0.3$, i.e. within the centre region, the difference between the measured chord length L_M and the length of the minor axis of a droplet/bubble L_{Ds} is small ($0.95 < L_M / L_{Bs} < 1.00$). When the probe pierces droplets/bubbles in the centre region, highly accurate measurement is achieved. In addition, the small difference between the minor-axis and measured chord lengths is a kind of random difference; therefore, it is very difficult to remove them from the measurement results.

書式変更: 両端揃え

書式変更: フォントの色: 自動

コメント [KN6]: WHAT small difference? You use the definitive article “the”, which implies the reader knows which difference. But it is not clear. Define it by saying “the small difference in ___s” OR even better, “the small difference in ___s between ___ and ___”

書式変更: フォントの色: 自動

書式変更: フォントの色: 自動

書式変更: フォントの色: 自動

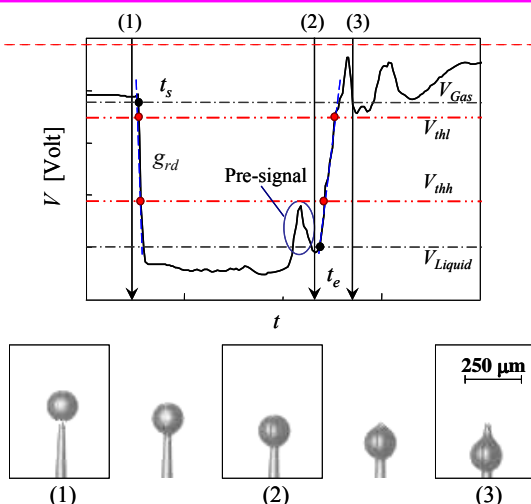


Figure 8. A typical signal in for droplet measurements via S-

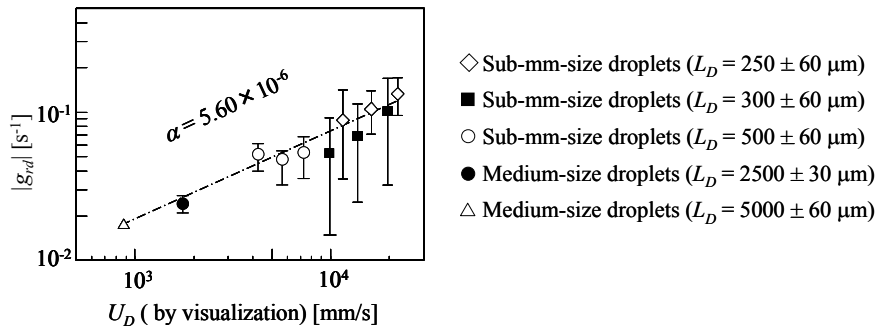


Figure 9. The relationship between g_{rd} and U_D (visualization) rearranged by using α of

Figure 11 shows snapshots ~~that in which~~ the fs-ProbeFs-TOP touches ~~on the one hand, the a~~ flat interface and ~~on the other,~~ a sub-mm-size droplet. In the cases of touching the flat interface at low velocity (~~a the~~ velocity of the probe is 100 mm/s), a large deformation is observed ~~on at~~ the gas-liquid interface as shown in ~~figureFig-~~ 11 (a). On the other hand, when the fs-ProbeFs-TOP touches a sub-mm-size droplet at a high velocity (10 m/s), the deformation of the droplet is very small as shown in ~~figureFig-~~ 11 (b). Hence, the deformation of the droplet does not become a serious problem when ~~we measure-measuring~~ tiny droplets moving at a high velocity. Unfortunately, this deformation ~~is was~~ not measured quantitatively. The deformation of the droplet ~~while~~ pierced by the probe is very small during measurement (between t_s and t_e), as shown in ~~the~~ snapshots of ~~figureFig-~~ 8. In the case of sub-mm-size droplet measurements, the deformation is smaller than 3.2 % of droplets' minor axes (this difference is a kind of bias), and in the case of ~~um-size micro size~~ droplet measurement it is smaller than 3.1 % of ~~the~~ droplets' minor axes (this difference is a kind of bias); i.e., the measurement is completed before large deformation. In fact, ~~as~~ the probe pierces the droplet in this region, highly accurate measurement is achieved. However, we need to know how to detect ~~the pierced~~ position ~~by of piercing~~ using the single-tip optical fibre probe, ~~to ensure that the probe has pierced the centre of the droplet.~~

書式変更: 両端揃え

書式変更: フォントの色 : 自動

コメント [KN7]: Is this what you mean?

書式変更: フォントの色 : 自動

書式変更: フォントの色 : 自動

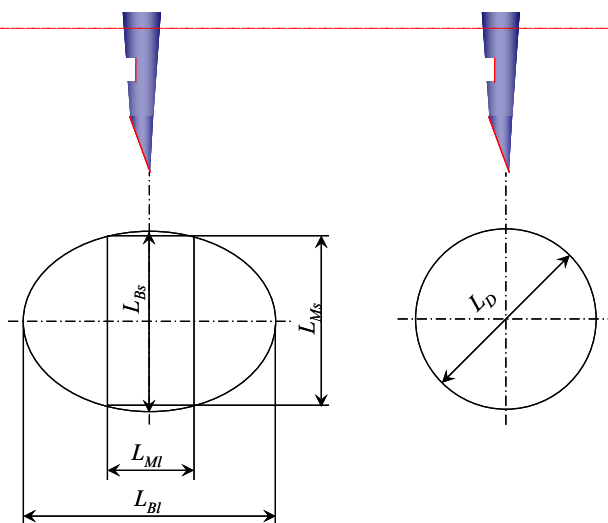
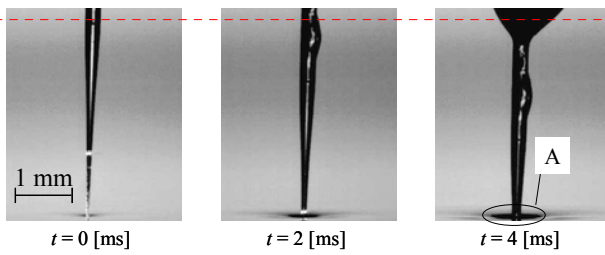
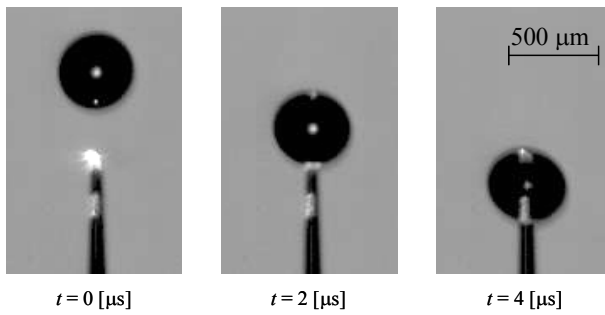


Figure 10. Schematic drawings of relationship between pierce region size and measurement chord length.



(a) **Snapshots:** The fs-Probe touching the a flat interface at a low velocity (100 mm/s); the fs-Probe touches the interface just at $t = 0$ [ms].



(b) **Snapshots:** The fs-Probe touching a sub-mm-size droplet moving at a high velocity (10 m/s);

Figure 11. Snapshots of touching process under different conditions.

We found ~~out~~ that a pre-signal appears only when ~~the wedge-shape tip of the both~~ either probe ~~(equipped with wedge shape tip)~~ pierces the centre region of a droplet/bubble. In ~~the case of~~ bubble measurement, most beams are emitted from the probe tip before they pierce ~~a the~~ bubble, because the probe tip is ~~eovered with~~ surrounded by liquid ~~phase~~ before ~~the detection of~~ encountering of the bubble. Hence, the emitted beams are reflected on the bubble frontal surface, and some of them re-enter ~~into~~ the probe; ~~this these~~ incident beams ~~are serve~~ as a pre-signal. On the other hand, in the droplet measurement, few beams are emitted from the probe tip; because the probe tip is ~~eovered with~~ surrounded by gas ~~phase~~ before ~~the detection of~~ encountering the droplet. Therefore, ~~the no~~ pre-signal ~~does not~~ appears before the detection of the droplet. However, ~~the a~~ pre-signal similar to the pre-signal of the bubble measurement appears just before the probe pierces the rear interface of the droplet only when the probe pierces the centre region.

In the measurement ~~by using a~~ single tip probe, this measurement method realizes ~~the high~~ accuracy measurement of the minor axes of ~~the~~ bubbles and droplets.

3.1.3 *Algorithm for S-TOP*. Figure 12 shows the algorithm for the processing of S-TOP signals. The signal processing is composed of four processes as described herein below: 1) the smoothing process, 2) the determination of thresholds, 3) the detection of event time and gradient of a burst signal, and 4) the calculation of chord length and velocity.

書式変更: 両端揃え

1) Smoothing process

The raw data of output signals are smoothed ~~via~~ by a 25-point moving average method to reduce the influence of high-frequency noise.

書式変更: 両端揃え

2) Determination of thresholds

We use the thresholds to accurately detect the event time. First, the maximum output voltage V_{max} and the minimum output voltage V_{min} are detected. Second, V_{Gas} and V_{Liquid} are calculated. In this study, V_{Gas} is the average value of the voltage over 90 %, and V_{Liquid} is the averaged value of the voltage under 10 %. Finally, the high threshold level V_{thh} and the low threshold level V_{thl} are decided. In this study, the high threshold level V_{thh} was 90 % of all the entire signal amplitude, and the low threshold level V_{thl} was 30 % of all the entire signal amplitude. These threshold values are decided by the results of comparison between the visualization and the probe signal. As a result, the difference of in detection of event time between the results of visualization and signal processing is less than 5% in all measurement cases. We consider this difference is as a kind of a bias difference (not random difference) in the calculation of event time; therefore, this bias is could be removed from the S-TOP measurement results.

書式変更: 両端揃え

コメント [KN8]: OR upper

コメント [KN9]: USE "lower" if you use "upper"

コメント [KN10]: Is this what you mean???

コメント [KN11]: See above.

3) Detection of event time and gradient of a burst signal

In this process, we detect the t_s and t_e , and calculate the gradient of the signal. First, the gradient of the falling edge and rising edge is calculated by equation (1), as shown in section 3.1.1. Next, we detect the duration time between the probe and a droplet. The event time t_s is defined as the intersection point of the straight line (i.e. the gradient is g_{rd}) and the gas-phase level at the falling edge. The event time t_e is defined as the intersection point of the straight line (i.e. the gradient is g_e) and the liquid-phase level at the rising edge. As a result,

書式変更: 両端揃え

we can calculate the event time. The bias (i.e. the difference is less than 5 % of the results via visualization) is considered in the calculation.

書式変更

書式変更: フォントの色 : 自動

4) Calculation of chord length and velocity

Finally, we calculate the droplet velocity and its chord length. In the calculation, we judge the pierced position. First, we calculate the droplet velocity by equation (2) as shown in section 3.1.1. The chord length L_D is calculated from equation (3) (shown in section 3.1.1). Next, we estimate the time range of generation of the pre-signal from droplet velocity and its diameter. We search for the pre-signal in this range by using a threshold. As part of this process, we can judge whether the probe pierces in the centre part of the droplet. Since When the probe pierces the centre part of a the droplet, we can measure the minor axes of the droplets. The pre-signal is described at in detail in section 3.1.2.

書式変更: 両端揃え

3.1.4 The algorithm for *fs-ProbeFs-TOP*. As shown in figure Fig- 13, the signal processing is composed of five processes as described below: 1) the smoothing process, 2) the histogram process, 3) the determination of thresholds, 4) the detection of event time and gradient of signal, and 5) the calculation of chord length and velocity.

書式変更: 両端揃え

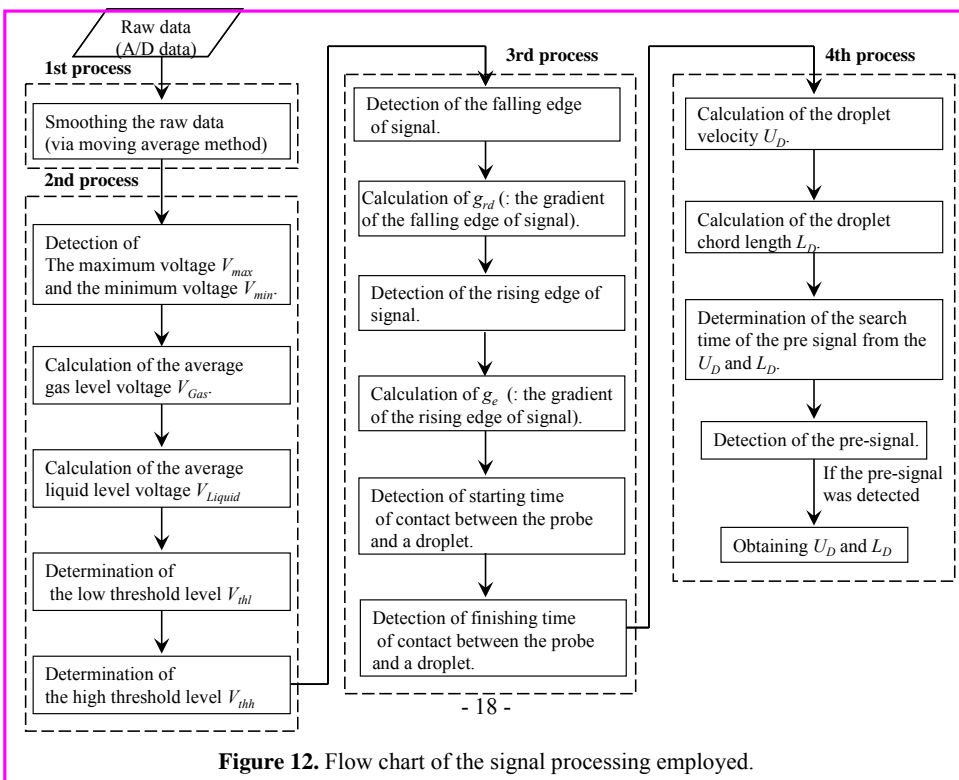


Figure 12. Flow chart of the signal processing employed.

~~in 2nd process: “The maximum voltage” → “The” should not be capitalized; “low threshold level” should be “lower threshold” and “high threshold” should be “upper threshold”. In 3rd process “start time” is better than “starting time”, don’t use “a” before droplet or “the” before probe in “between probe and droplet”. In 4th process, don’t use “the” before U and L; use present tense “if pre signal is detected”.~~

Fig. 4: The typical S-TOP signal and snapshots corresponding to the signal showing the contact process between a sub-mm-sized droplet and the S-TOP probe.

1) Smoothing process

The raw data of the output signals are smoothed ~~viaby the~~ 25-point moving average method to reduce the influence of high-frequency noise.

2) Histogram process

The histogram method (Sakamoto and Saito) is employed to accurately detect the output voltage levels.

We obtain ~~the a~~ histogram of ~~the~~ output voltage signal. The threshold values ~~which that~~ we want can be easily extracted from peak values of the histogram. Figure 14 shows an example of the histogram of ~~fs-ProbeFs-TOP~~ signals. ~~Clear f~~Four ~~clear~~ peaks (marked in the figure) are detected from the histogram. Each peak corresponds to ~~the a~~ stable output voltage level of ~~the fs-ProbeFs-TOP~~ signal:

- (1) Full gas-phase level (both probe tip and groove are ~~positioned~~ in air) = V_{Gas} ,
- (2) Tip level (only the probe tip is positioned in the droplet) = V_{tl} ,
- (3) Full ~~l~~iquid-phase level (both ~~of~~ the probe tip and the groove are ~~covered within~~ the droplet) = V_{Liquid} ,
- (4) Groove level (the groove ~~is~~ in the droplet) = V_{gl} .

書式変更: フォントの色 : 自動

3) The determination of thresholds

We use the thresholds to accurately detect the event time in each level as shown in ~~figure Fig.~~ 14.5. We decide the ~~upper (V_{th1}) and lower (V_{tl})~~ first threshold levels to ~~detect-determine~~ the start~~ing~~ time of contact between the ~~fs-ProbeFs-TOP~~ and a droplet. ~~The first high threshold level V_{th1} and the first low threshold level V_{tl} are decided.~~ In this study, V_{th1} was 90 %, and V_{tl} was 30 % of ~~the difference in the~~ signal amplitude between V_{Gas} and V_{tl} . ~~Next, the upper (V_{th2}) and lower (V_{th2}) second threshold levels are determined in order to detect the time the droplet touches the groove edge; here, the upper threshold level V_{th2} was 90 %, and the lower threshold level V_{th2} was 20 % of the signal amplitude between V_{Liquid} and V_{tl} . Finally, the upper (V_{th3}) and lower (V_{th3}) third threshold levels are determined in order to detect the end time of contact between the ~~fs-ProbeFs-TOP~~ and the droplet; here, the V_{th3} was 90 %, and V_{th3} was 20 % of the signal amplitude between V_{Liquid} and V_{gl} . ~~The second threshold level is decided in order to detect the time of the droplet touching the groove edge. The second high threshold level V_{th2} and the second low threshold level V_{th2} are decided. The high threshold level V_{th2} was 90 %, and the low threshold level V_{th2} was 20 % of signal amplitude between the V_{liquid} and V_{tl} . Finally, the third threshold level is decided in order to detect the finishing time of contact between the fs-Probe and the droplet. The third high threshold level V_{th3} and the third low threshold level V_{th3} are decided.~~~~

書式変更: 両端揃え

コメント [KN12]: Is this what you mean? Otherwise, I don't understand "signal amplitude between..."

コメント [KN13]: See above.

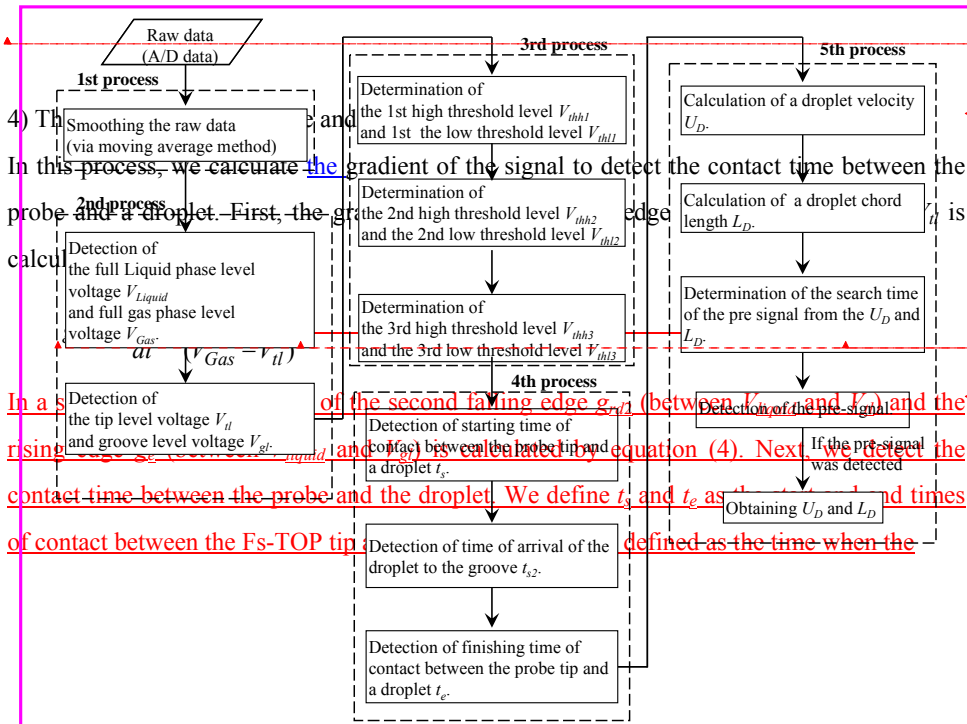
コメント [KN14]: See above.

~~2nd process: "Liquid" should not be capitalized, also don't need the paragraphing in that box. 3rd process: suggest "upper" instead of "high" threshold and "lower" for "low". 4th process: suggest "start time" and "end time". 5th process: delete "a" from the phrases "droplet velocity", "droplet chord length"; delete "the" from "the U"~~

書式変更: 単語の途中で改行する

V_{thh3} was 90 %, and V_{thl3} was 20 % of signal amplitude between the V_{liquid} and V_{gt} . The difference of in detection of event time between the results of visualization and this signal processing is was less than 5.5 % in all measurement cases. We consider this difference in the calculation of the event time is as a kind of a bias difference (not a random difference); therefore, this bias is could be removed from the measurement results viaby fs-ProbeFs-TOP.

書式変更: 両端揃え



書式変更: フォントの色 : 自動

書式変更: フォントの色 : 自動

書式変更: 両端揃え

書式変更: フォントの色 : 自動

書式変更: フォントの色 : 自動

書式変更: フォントの色 : 自動

書式変更: 両端揃え

Figure 13. Flow chart of the signal processing of the fs-ProbeFs-TOP.

droplet touches the groove edge. The event time t_s is defined as the intersection point of the

コメント [KN15]: OR "the duration of the droplet touching the groove edge" ?

書式変更: フォントの色 : 自動

書式変更: フォントの色 : 自動

書式変更: フォントの色 : 自動

書式変更: フォントの色 : 自動

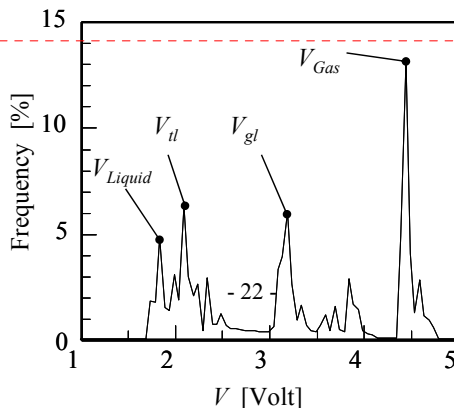


Figure 14. An example of the histograms of output voltage of fs-Probe signals.

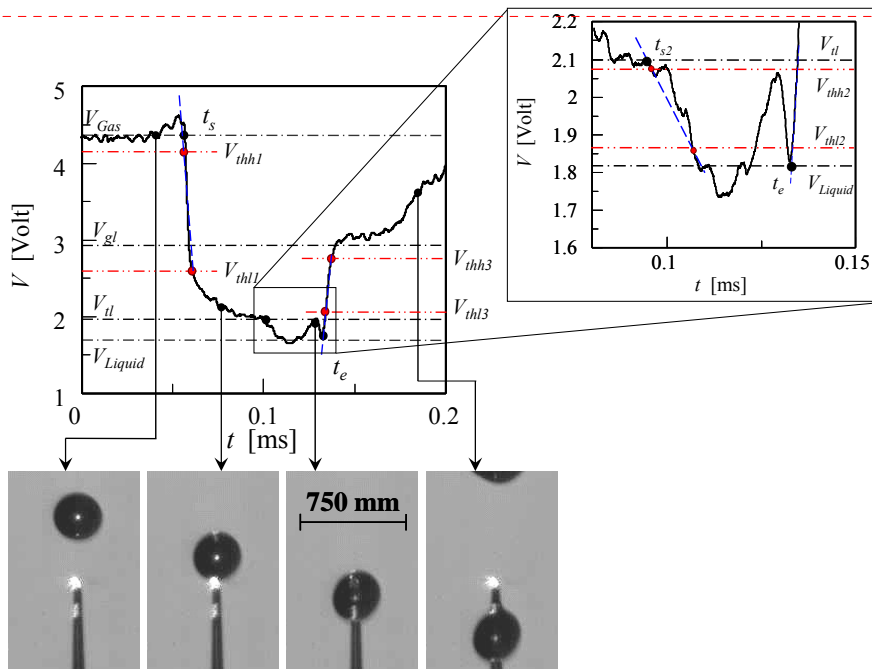


Figure 15. Schematic diagram of signal processing for fs-Probe.

In a similar way, the gradient of the second falling edge g_{rd2} (between V_{liquid} and V_{it}) and the rising edge g_e (between V_{liquid} and V_{gt}) is calculated by equation (4). Next, we detect the contact time between the probe and the droplet. We define t_s and t_e as the beginning start and finishing end times of contact between the probe tip and the droplet. The t_{s2} is defined as the time when the droplet touches the groove edge. The t_e is defined as time of the droplet touching the groove edge. The event time t_s is defined as an the intersection point of the straight line (i.e. the gradient is g_{rd}) and the gas-phase level at the first falling edge. An The intersection point of the straight line (i.e. the gradient is g_{rd2}) and the gas-phase level at the second falling edge is defined as the event time t_{s2} . The event time t_e is defined as an the intersection point of the straight line (i.e. the gradient is g_e) and the liquid-phase level at the rising edge. As a result, we can detect event time in with high accuracy (the difference is less than 5.5 % as described in the above).

書式変更: 両端揃え

コメント [KN16]: OR “the duration of the droplet touching the groove edge”?

5) Calculation of chord length and velocity

Finally, we calculate the droplet velocity and its chord length, and we judge the pierced position of piercing by the probe based on the pre-signal. First, we calculate the droplet velocity by equation (5):

$$U_D = \frac{L_P}{(t_{s2} - t_s)} \quad (5)$$

書式変更: 両端揃え

変更されたフィールド コード

where L_P is ~~a~~the distance between the tip point and the groove. The chord length L_D is calculated from equation (6),

$$L_D = U_D \times (t_e - t_s). \quad (6)$$

Next, we judge whether the probe pierces ~~in~~the centre part of the droplet by using the pre-signal (the algorithm is described in section 3.1.3, and the pre-signal is described in section 3.1.2).

4. Results and Discussion

4.1 The S-TOP measurements.

4.1.1 Characteristics of the S-TOP signals. The output signals in the S-TOP measurements of various diameter droplets are shown in ~~figure~~Fig. 16. When the sub-mm-size droplet contacts ~~with~~the S-TOP, the output signal corresponding with the liquid-phase level does not stabilize. Since the S-TOP diameter is inadequate in comparison with the droplet diameter, the smallest output becomes large with a decrease in the droplet diameter. Hence, the liquid does not ~~cover~~surround the sensor section of S-TOP completely. Therefore, the output voltage corresponding ~~with~~to the liquid-phase tends to be high when the droplet diameter is small. The typical output signals of the S-TOP and the corresponding pictures during ~~its~~the penetration process are shown in ~~figure~~Fig. 17. In ~~figure~~Fig. 17 (a), the output signal changes in two stages for successional penetration of two droplets. The output voltage of the S-TOP signal decreases with the penetration of the first droplet. Before the signal is restored to the gas-phase level, the signal again decreases due to the penetration of the next droplet. Therefore, the output voltage of the S-TOP decreases from the liquid-phase level of the ~~precedent~~preceding droplet. We consider that this phenomenon is caused by a liquid-phase thin film ~~which is~~ formed on the S-TOP surface when the first droplet hits the S-TOP. ~~Then~~The next droplet hits the S-TOP before the removal of the liquid thin film. In addition, in these measurements the amplifier frequency of the photo-multiplier is 20 kHz. This frequency

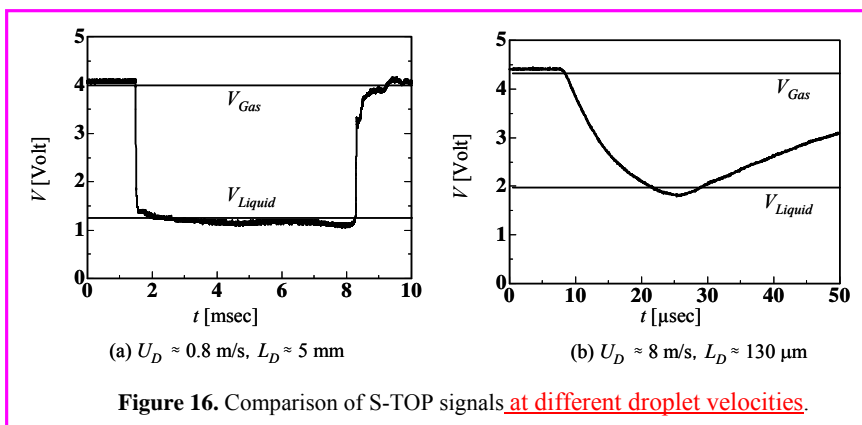
is too low to detect a pre-signal; therefore, no pre-signal is observed in the sample signals in [figure Fig. 17](#) (in order to detect a pre-signal, a frequency of 200 kHz is required).

4.1.2 Comparison between S-TOP and visualization results. Figure 18 shows [the a](#) comparison between the results measured by the S-TOP and those obtained from [the](#) visualization. In this study, we measured two hundred sub-mm-size droplets to evaluate [the](#) measurement accuracy of S-TOP. The average droplet velocities [via-measured by](#) S-TOP ([figure Fig. 18 \(a\)](#)) [showed satisfactory agreement](#) with those from the visualization; [satisfactorily](#). The difference [of-in](#) averaged velocity between the S-TOP [calculation](#) and visualization [is-was](#) less than 7.2 %. However, the droplet velocities measured by S-TOP have a large dispersion compared with those by the visualization. [The dispersion, with a](#) ranges from $\pm 30\%$ to $\pm 60\%$ of droplet velocities. Furthermore, this dispersion does not depend on the droplet velocity. Figure 18 (b) shows [the a](#) comparison of the droplet chord lengths between the S-TOP and the visualization. The average chord lengths [viaby](#) S-TOP are larger than those from the visualization. Furthermore, the [dispersiontribution](#) ranges from 30 % to 60 %. In the visualization, we obtained the barycentric velocity of the droplets. On the other hand, the S-TOP measured the interface velocity of the droplets. Therefore, the difference between the S-TOP and [the](#) visualization results includes [a kind of](#) random differences ([not-as opposed to bias differences](#)) due to uncertain factors (e.g., the primary surface oscillations of the droplets). It is difficult to [remove-completely remove this-these](#) random differences from the measurement results of S-TOP. Based on our results, the number of samples should be larger than 200. ([In addition, in](#) these average results, the bias differences described in 3.1.2 [are not removed.](#))

書式変更: 両端揃え

コメント [KN17]: Why do you use “distribution” here and “dispersion” for velocity? “Distribution is the more common statistical term.”

コメント [KN18]: Do you mean “should not be”? Or are you just informing reader (if so, keep as is)



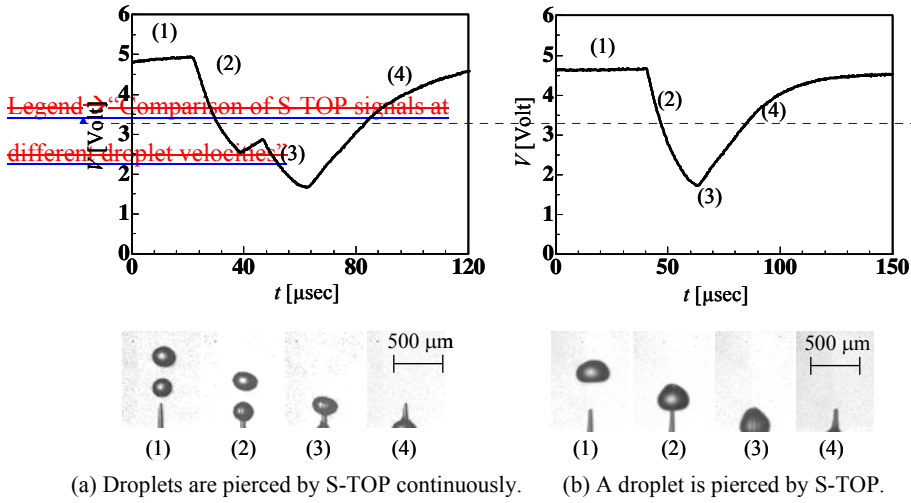


Figure 17. Typical samples of S-TOP signals.

~~Matsuda & Saito~~ MST/307768

書式変更: 単語の途中で改行する

4.2 ~~fs-Probe~~Fs-TOP measurement.

4.2.1 Comparison between *fs-ProbeFs-TOP* and visualization results (mm-size droplets). The droplet velocity calculated from equation (5) and the chord lengths calculated from equation (6) were compared with those obtained from the visualization. The droplet chord lengths from the visualization were calculated based on the projected areas. The comparison is listed in Table 1 and summarised in figure Fig- 19. The *fs-ProbeFs-TOP* results on-for droplet velocities and chord lengths are less than those from the visualization. When the droplet velocities are smaller than 2.0 m/s, the droplet velocities via-by *fs-ProbeFs-TOP* is-are approximately 5 % (bias difference) smaller than those via-by visualization. However, when the droplets velocities are higher than 2.0 m/s, those via-by *fs-ProbeFs-TOP* are approximately 10 % (bias difference) smaller than those via-by visualization. The number of samples was random 10 of 100. The dispersion of the other 10 samples has-had the-a similar distribution. The dispersion observed in the droplet velocities rangeds from $\pm 12\%$ (at 2 m/s) to $\pm 20\%$ (at 0.26 m/s). This dispersion decreases with increase in droplet velocity. This property is very different from the-that of S-TOP (see 4.1.2).

書式変更: 両端揃え

コメント [KN19]: ? wouldn't it be the other 90 samples? OR "Another 10 samples that were measured had a"

コメント [KN20]: Again, you use "distribution" for chord length and "dispersion" for velocity. I don't see why the term should be different.

The chord lengths measured by *fs-ProbeFs-TOP* include the randomness due to piercing position (however within the centre region of the droplets) and those due to the surface oscillation. Furthermore, they include randomness propagated from velocities; the chord length is calculated from velocity (equation (6)). The chord lengths obtained from the visualization include randomness due to the surface oscillation. Figure 19 (b) shows the-the relation of comparison of chord-length dispersion to droplet velocity for both-between the *fs-ProbeFs-TOP* and the visualization, against the droplet velocity. The dispersion of the *fs-ProbeFs-TOP* results is wider than that of the visualization. The dispersion is not influenced by the velocity.

4.2.2 Comparison between *fs-ProbeFs-TOP* and visualization results (sub-mm-size and μm -size droplets). The comparison of measurement results of-for sub-mm-size droplets between-by *fs-ProbeFs-TOP* and visualization is-are listed in Table 2 and also summarised in figure Fig- 20. The average results of the *fs-ProbeFs-TOP* on-for droplet velocities and chord lengths are-were approximately 10 % less than those from the

書式変更: 両端揃え

書式変更: フォントの色 : 自動

書式変更: フォント : 斜体, フォントの色 : 自動

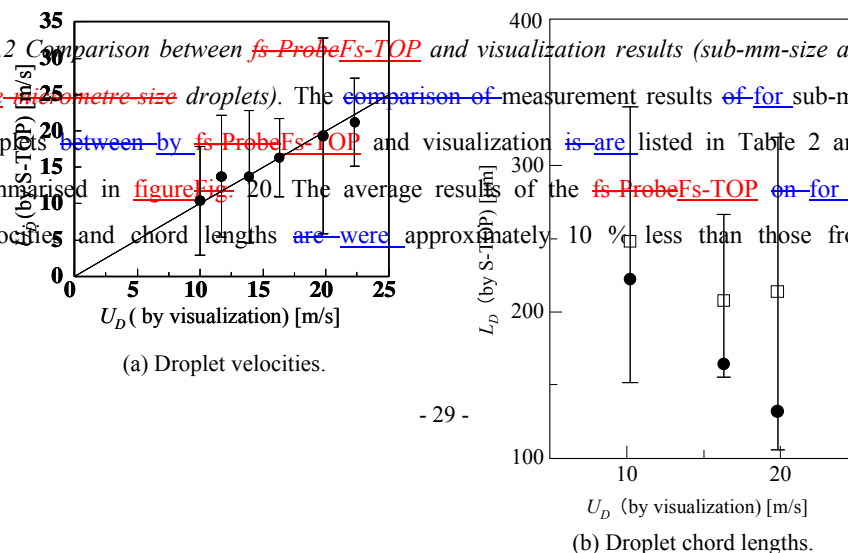


Figure 18. Differences between S-TOP and visualization results.

visualization (this difference is a kind of bias). The velocity dispersion of ~~fs-ProbeFs-TOP~~ (figureFig. 20) ~~is-was very-much~~ smaller than that ~~viaby~~ S-TOP (see figureFig. 18). From figureFig. 20, the velocity dispersion of ~~the fs-ProbeFs-TOP~~ decreases with ~~the~~ increase in ~~the~~ droplet velocity even in sub-mm-size measurements. Those tendencies of the measurement results of the sub-mm-size droplets are the same tendency ~~of-for~~ those of the mm-size droplets. However, the dispersion of the measurement results of sub-millimetre droplets is smaller than ~~those-that~~ of ~~the~~ millimetre-size droplets. ~~(In-addition,-i)~~In these average results, the bias differences described in 3.1.2 are not removed.)

Measurement results of the ~~um-size-micrometre-size~~ droplets are shown in figureFig. 21. The results of droplet velocity ~~via-by fs-ProbeFs-TOP~~ are smaller than those ~~of-theby~~ visualization. Furthermore, the measurement results of the droplet chord lengths are also smaller than those from the visualization. ~~(In these average results, the bias differences described in 3.1.2 are not removed.)~~ Considering that S-TOP can not measure ~~um-size-micrometre-size~~ droplets, the ~~fs-ProbeFs-TOP~~ ~~has-demonstrated~~ satisfactory performance ~~of-in~~ measuring velocities and chord lengths of ~~um-size-micrometre-size~~ droplets.

5. Conclusion

~~In this paper, we describe the characteristics and performance of the Fs-TOP, a newly developed single-tip optical fibre probe micro-processed by femtosecond pulse laser. We also~~

4. Conclusion

In this paper, we described the characteristics and performance of the S-TOP and fs-Probe (a newly developed single-tip optical fibre probe micro-processed by femtosecond-pulse laser). We also compared the characteristics of the fs-Probe, S-TOP and S-TOP in detail, in order to present guidelines in order to allow researchers in various fields to select for effective the appropriate probe for a particular applications of those to various targets. Their characteristics, performance and measurement accuracies were evaluated based on the comparisons of the probe measurement results between the S-TOP/fs-Probe and with

visualization results. The ~~fs-Probe~~Fs-TOP has satisfactory performance and accuracy for measurements of ~~um-size-micrometer-size~~ droplets. Our investigation is summarized as follows.

For the specific purpose of ~~reduc~~ing~~tion-of~~ the random errors due to piercing position, we proposed a new method using a pre-signal to detect whether the S-TOP/~~fs-Probe~~Fs-TOP pierces the centre region of a droplet/bubble ~~by using the pre-signal~~. The random errors are less than 5 % of the minor axes of ~~the~~ droplets with 50 μm – 2 mm in equivalent diameter.

The forced surface deformation of the droplet when the probe touches the droplet surface is very small for droplets ~~with~~ 50 – 500 μm in equivalent diameter. Hence, this surface deformation is negligible for the droplets in ~~the above~~this diameter range.

The deformation of ~~the a~~ droplet pierced by ~~the either~~ probes is very small during measurement. In the case of sub-mm-size droplet measurements, the deformation is ~~smaller~~ less than 3.2 % of droplets' minor axes (~~this a bias~~ difference ~~is a kind of bias~~), and in the case of ~~um-size-micro-size~~ droplet measurement, it is smaller than 3.1 % of droplets' minor axes (~~this difference is a kind of a~~ bias difference).



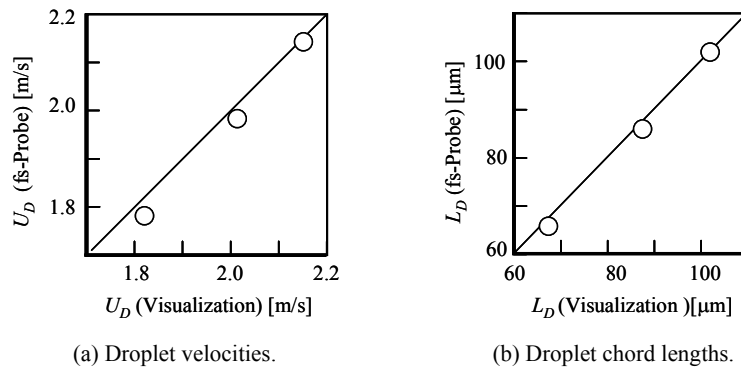


Figure 21. Comparison of fs-Probe measurement results of micrometre-size droplets between fs-Probe and visualization results.

On the basis of these results, first, we described the characteristics and performance of S-TOP. In the measurement of sub-mm size droplet, s, the difference of in averaged velocity between the S-TOP and visualization is less than 7.2% (in these average results, the bias differences described in above are not removed). However, the droplet velocities and chord lengths

measured by S-TOP have a large dispersion compared with those by the visualization. The dispersion ranges from $\pm 30\%$ to $\pm 60\%$ of droplet velocities. Furthermore, the average chord lengths via S-TOP are larger than those from the visualization. In addition, those distribution ranges are also from 30% to 60%. As the reason of this, the S-TOP measured the interface velocity (not barycentric velocity) of the droplets. Therefore, the difference between the S-TOP and visualization results includes a kind of random differences (not bias) due to uncertain factors (e.g., the primary surface oscillations of the droplets). It is difficult to remove completely this random difference from the measurement results of S-TOP. Based on our results, we suggested that the number of samples of the S-TOP measurement should be larger than 200 to measure the droplets in order to obtain high accuracy results. Next, we described the performance and properties of the S-TOP/fs-Probe by examining mm-size droplets, and sub-mm size droplet. The dispersion of the measurement results of sub-mm size droplets is smaller than that of mm size droplets. In the measurement of sub-mm size droplets, the average results of the fs-Probe for droplet velocities and chord lengths were approximately 10% less than those from the visualization (this is a bias difference, a kind of bias). Moreover, the velocity dispersion of the fs-Probe is much smaller than that via S-TOP. The velocity dispersion of fs-Probe decreases with an increase in the droplet velocity, in both of the mm-size droplet and sub-mm size droplet measurements.

In addition, we demonstrated the measurement of velocities and chord lengths of micrometre-size droplets using the fs-Probe. The results of droplet velocity via fs-Probe are smaller than those of the visualization. Furthermore, the measurement results of the droplet chord lengths are also smaller than those from the visualization (in these average results, the bias differences described in above are not removed). Considering that S-TOP can not measure micrometre size droplets, the fs-Probe has demonstrated satisfactory performance of measuring velocities and chord lengths of micrometre size droplets.

As above, each optical probe (S-TOP/fs-Probe) has different kinds of characteristics. In this paper, we clarified the application range of S-TOP and fs-Probe quantitatively as follows:

コメント [KN21]: Why do you use +/- here and not below?

書式変更: フォントの色: 黒

- 1) The measurement object of the S-TOP is the a sub-mm size droplet moving less than 5 m/s. In the cases of measuring the meent of averaged velocity of sub-mm size droplets, the desirable sample number of for the S-TOP is larger greater than 200.
- 2) The measurement object of the fs Probe is the micrometre size droplet and sub-mm size droplets moving at over speeds of 5 m/s or more. In the cases of measurement of measuring the averaged velocity of sub-mm size droplets, the desirable sample number of for the fs Probe is more greater than 10.

Nomenclature

g_{rd}	gradient of the S-TOP signal (s^{-1})
L_D	chord length pierced by Probe (mm or μm)
L_P	length between tip and groove of the fs-Probe <u>Fs-TOP</u> (mm or μm)
t	time (s or ms)
V	output of a photo multiplier (V)
U_D	interface velocity (m/s or mm/s)

Greek symbol

α	proportionality coefficient (m)
----------	---------------------------------

Subscripts

2	at groove
f	end of contact
Gas	gas phase level
Liquid	liquid phase level
min	minimum output
s	start of contact

References

~~Abuaf N., Jones O. C. Jr. and Zimmer A., 1978; Optical probe for local void fraction and interface velocity measurements, *Review of Scientific Instruments*, Vol. 49, 1090-1094.~~

~~Cartellier A., 1990; Optical probes for local void fraction measurements: Characterization of performance, *Review of Scientific Instruments*, Vol. 61, 874-886.~~

~~Cartellier A. and Achard, J. L., 1991; Local phase detection probes in fluid/fluid two-phase flows; *Review of Scientific Instruments*, Vol. 62, 279-303.~~

~~Cartellier A., 1992; Simultaneous void fraction measurement, bubble velocity, and size estimate using a single optical probe in gas-liquid two-phase flows; *Review of Scientific Instruments*, Vol. 63, 5442-5453.~~

~~Cartellier A., 1998; Measurement of gas phase characteristics using new monofibre optical probes and real-time signal processing; *Nuclear Engineering and Design*, Vol. 184, 393-408.~~

~~Clark N. N., Liu W. and Turton R., 1996; Data interpretation techniques for inferring bubble size distribution from probe signals in fluidized systems, *Powder Technology*, Vol. 88, 179-188.~~

~~Clark N. N. and Turton R., 1988; Chord length distributions related to bubble size distributions in multiphase flows; *International Journal of Multiphase Flow*, Vol. 14, 413-424.~~

~~Hong M., Cartellier A., and Hopfinger E. J., 2004; Characterization of phase detection optical probes for the measurement of the dispersed phase parameters in sprays; *International Journal of Multiphase Flow*, 30 615-648.~~

~~Matsuda & Saito MST/307768~~

書式変更: 単語の途中で改行する

~~Mudde R F and Saito T 2001 Hydrodynamical similarities between bubble column and bubbly pipe flow J. Fluid Mech. 203-228~~

書式変更: フォントの色 : 自動

~~Saito T, and Mudde R- F, 2001, Performance of 4-tip Optical Fibre Probe and Bubble Characterizations by the Probe in Turbulent Bubbly Flows, Proceedings of International Conference on Multiphase Flow 2001, Paper No.111, in CD-ROM.~~

~~Saito T, Ishigaki Y, and Mizuno Y, 2004, Measurement and Characterization of Bubbles in a Bubble Column using 4-Tip Optical Fibre Probe, Proceedings of International Conference on Multiphase Flow 2004, Paper No.113, in CD-ROM.~~

~~Saito T, Kitamura M, Kajishima T, and Hatano H, 1999, Measurement of bubble dynamics by an optical fibre probe (1st Report), Influence of an optical fibre probe on bubble interfacial motion, Transactions of Japan Society of Mechanical Engineers Series B, 65 -2619-2626 (in Japanese).~~

書式変更: フォント : 斜体 (なし)

~~Saito T, and Kajishima T, 2002, Measurement of bubble dynamics by an optical fibre probe (2nd Report), simultaneous measurement of interfacial velocity and chord length of a bubble, Transactions of Japan Society of Mechanical Engineers Series B, 68 -2719-2725 (in Japanese).~~

書式変更: フォント : 斜体 (なし)

~~Saito T 2000 Japanese Patent No. 3018178~~

~~Saito T, 2007a Japanese Patent, Patent application number 177607, 2007.~~

~~Saito T, Japanese Patent, No. 3018178, 2000.~~

~~Saito T, 2007b Tiny Bubbles and Droplets Measurement by Optical Fibre Probe Processed Using a Femtosecond Pulse Laser, Proceedings of International Conference on Multiphase Flow 2007, Key note lecture, Paper No. KN 10, in CD-ROM.~~

~~Matsuda & Saito~~ MST/307768

書式変更: 単語の途中で改行する

Saito T; 2007; Bubble and droplets measurement via optical fibre probe processed by femtosecond pulse laser; *Proc. eedings of International Conf. erence on Nuclear Engineering 16*, Paper No. 48470, in CD-ROM

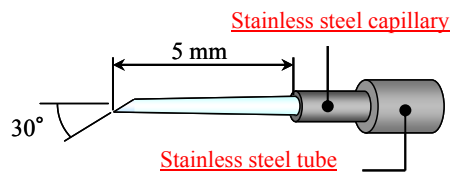


Figure 1. Structure of S-TOP.

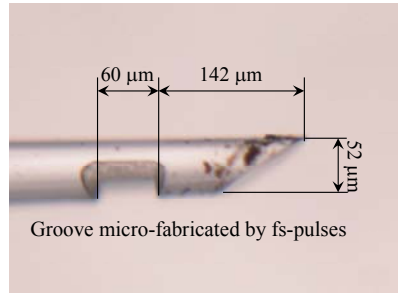


Figure 2. Close-up photograph of ~~fs-~~
~~Probe~~Fs-TOP for sub-mm-size droplets.

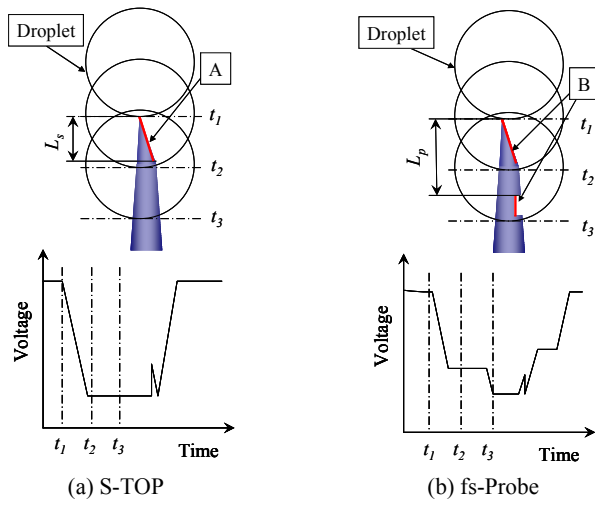


Figure 3. Schematic diagram of measurement processes of the S-TOP and fs-Probe.

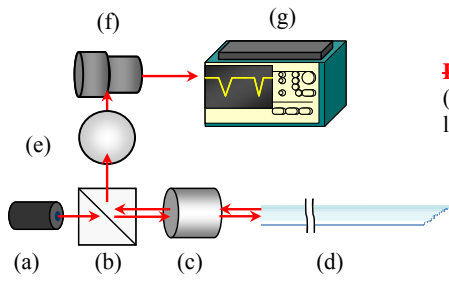
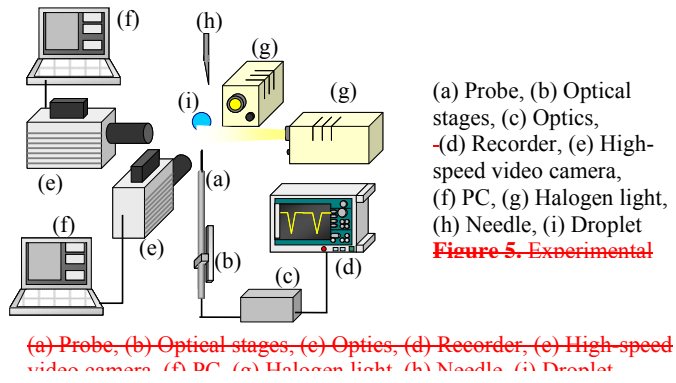
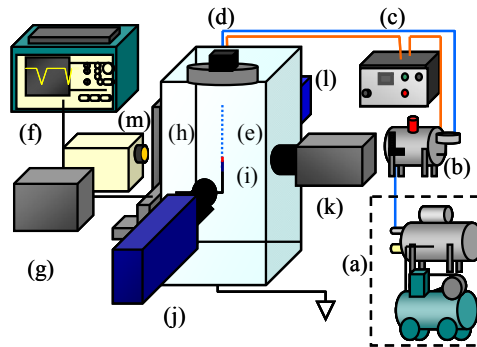


Figure 4. Optics.
(a) Laser diode, (b) Beamsplitter, (c) Objective lens, (d) Optical fibre probe, (e) Polarizer,

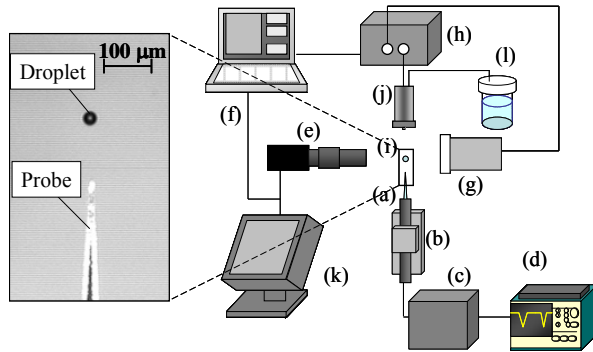
Figure 4. Optics.





(a) Pressurization source, (b) Water tank, (c) Pressure controller, (d) Electromagnetic valve, (e) Piezo nozzle, (f) Digital oscilloscope, (g) Optical system, (h) 3-axis unit, (i) S-TOP, (j) High-speed video camera 1, (k) High-speed video camera 2, (l) Strobe light, (m) Halogen light source.

Figure 6. Experimental setup for measurement of sub-millimetre-size droplets.



(a) Probe, (b) Optical stages, (c) Optical system, (d) Digital oscilloscope,
(e) High-speed video camera, (f) PC, (g) Strobe light, (h) Piezoelectric ink jet nozzle,
(i) Droplet,
(j) Controller, (k) Monitor, (l) Water tank

Figure 7. Experimental setup for measurement of μm ierometre-size droplets.

(a) Probe, (b) Optical stages, (c) Optical system, (d) Digital oscilloscope,
(e) High speed video camera, (f) PC, (g) Strobe light, (h) Piezoelectric ink jet nozzle, (i)
Droplet,
(j) Controller, (k) Monitor, (l) Water tank

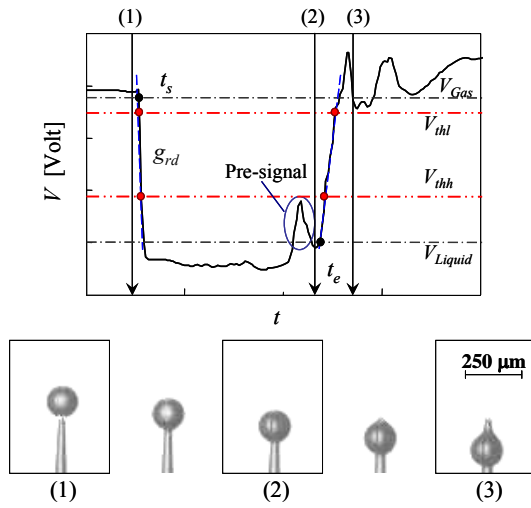


Figure 8. A typical signal [in-for](#) droplet measurements [via](#)by S-

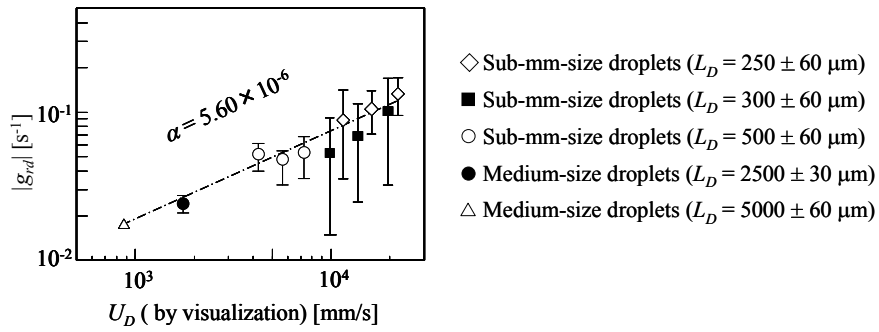


Figure 9. The relationship between g_{rd} and U_D (visualization) rearranged by using α of

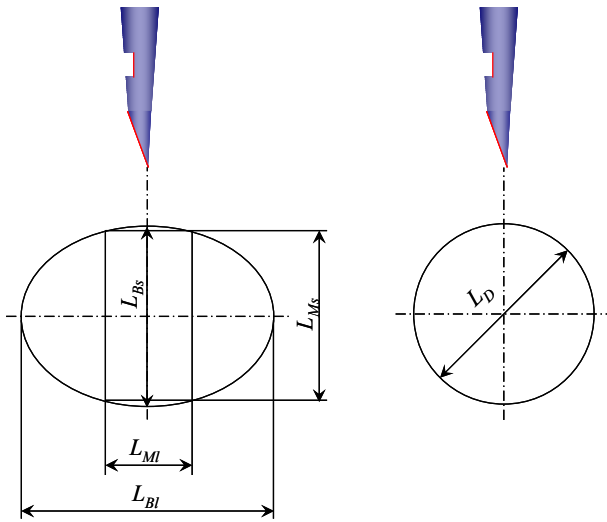
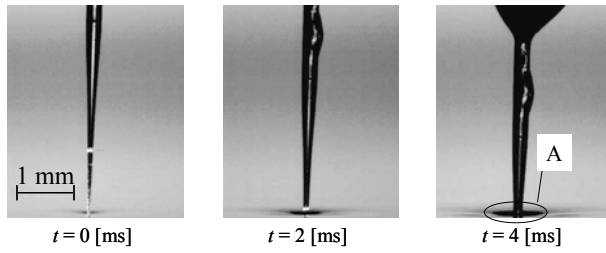
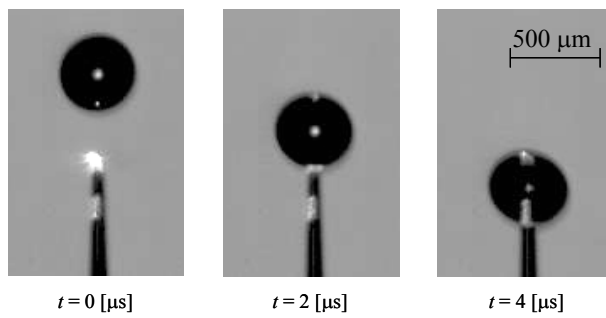


Figure 10. Schematic drawings of relationship between pierce region and measurement chord length.



(a) Snapshots: The fs-Probe touching the a flat interface at a low velocity (100 mm/s);



(b) Snapshots: The fs-Probe touching a sub-mm-size droplet moving at a high velocity (10m/s);

Figure 11. Snapshots of touching process under different conditions.

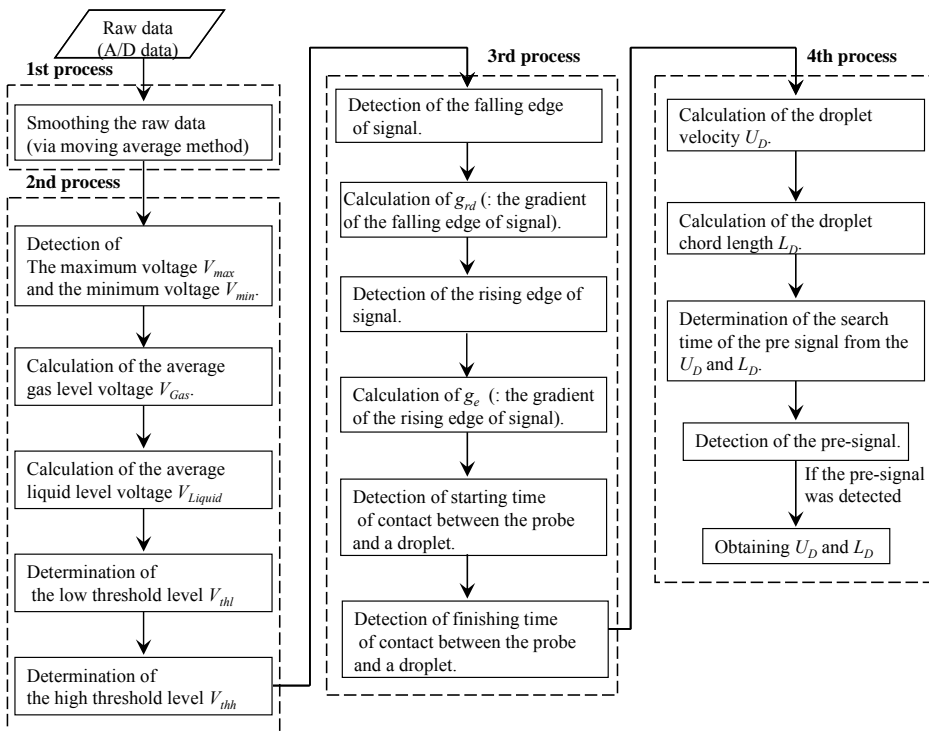


Figure 12. Flow chart of the signal processing employed.

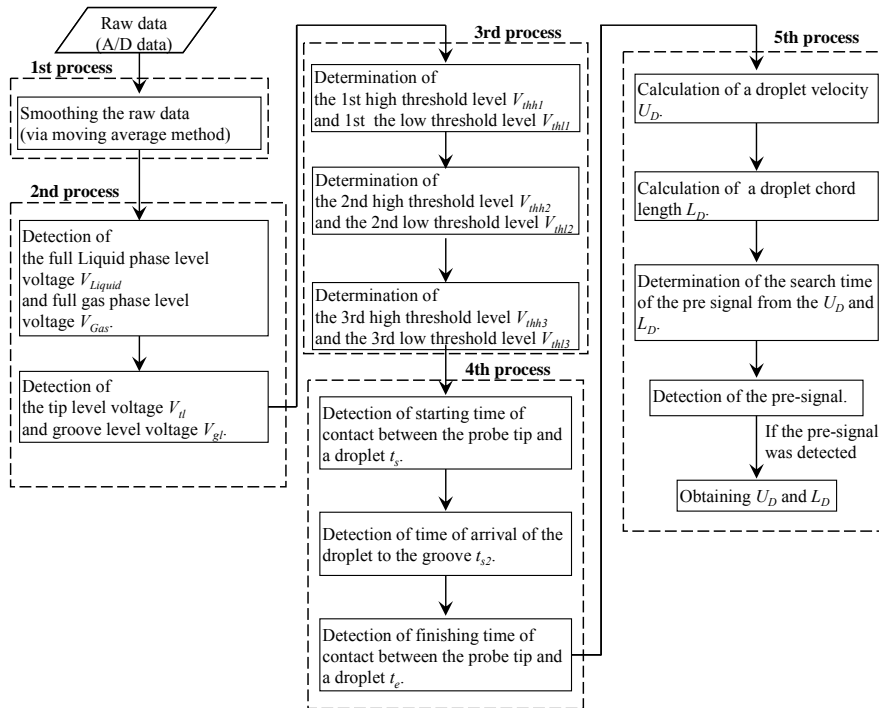


Figure 13. Flow chart of the signal processing of the ~~fs-ProbeFs-TOP~~.

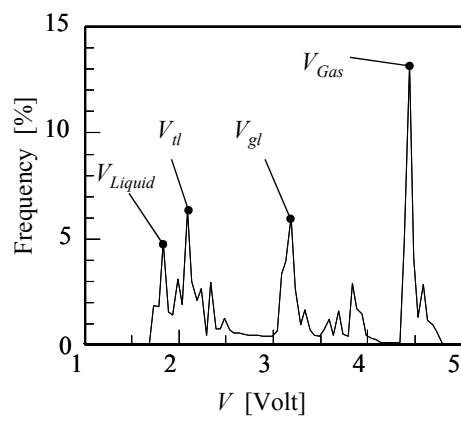


Figure 14. An ~~example~~ ~~sample~~ of the histograms of output voltage of fs-Probe signals.

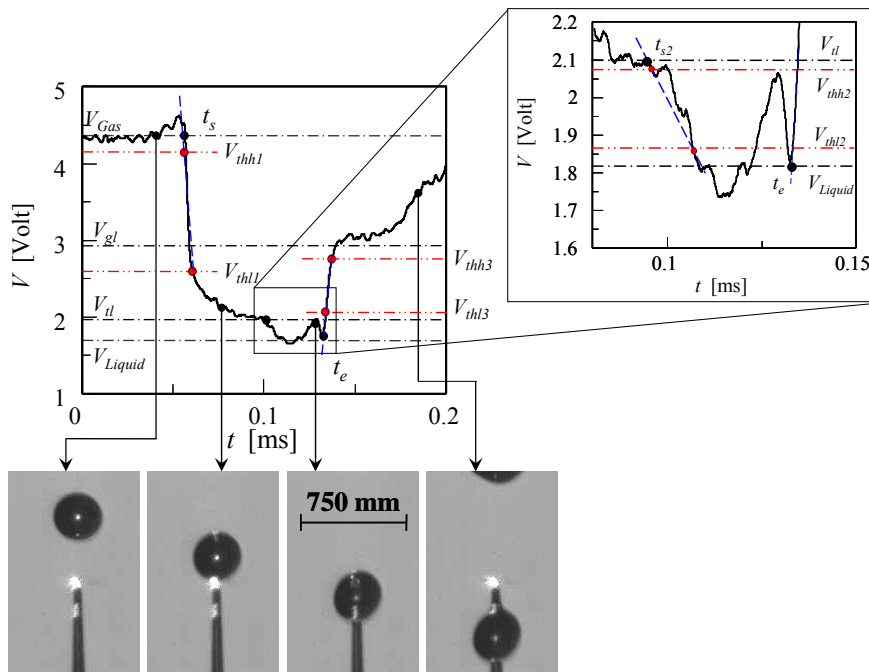
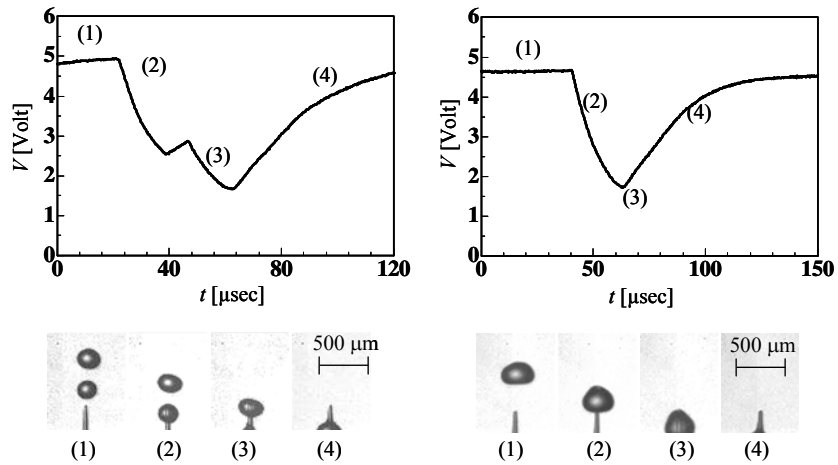


Figure 15. Schematic diagram of signal processing for fs-Probe.



(a) Droplets are pierced by S-TOP continuously. (b) A droplet is pierced by S-TOP.

Figure 17. Typical samples of S-TOP signals.

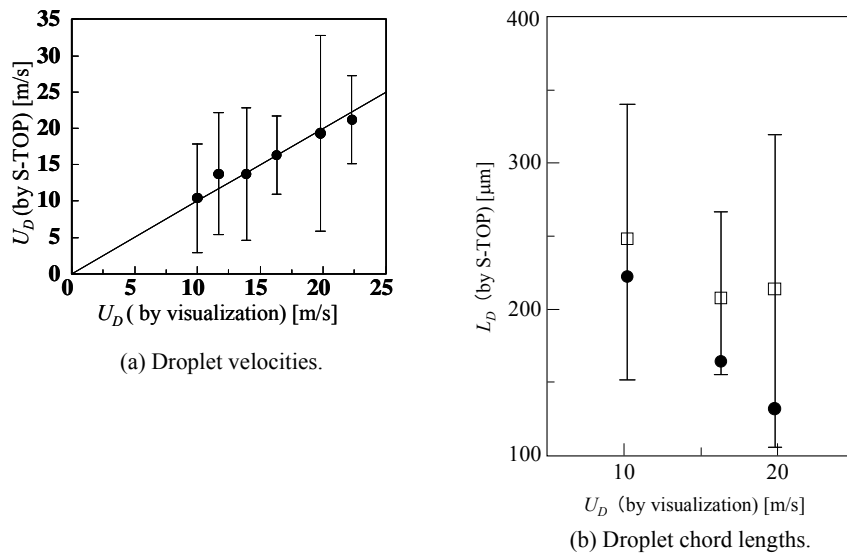


Figure 18. Differences between S-TOP and visualization results.

Table 1. Differences between ~~fs-Probe~~Fs-TOP and visualization results (mm-size droplets).

(a) Average droplet velocities

Visualization [m/s]	fs-Probe [m/s]	Differences [%]
0.279	0.271	-2.8
0.681	0.653	-4.3
1.069	1.040	-2.8
1.434	1.350	-6.2
1.776	1.691	-5.0
2.210	1.989	-11.1

(b) Average droplet chord lengths

Velocities [m/s]	Visualization [mm]	fs-Probe [mm]	Differences [%]
0.28	2.89	2.48	-16.3
0.68	2.65	2.77	4.2
1.07	2.77	2.53	-9.5
1.43	2.20	2.48	11.4
1.78	2.79	2.68	-4.1
2.21	2.21	2.04	-8.6

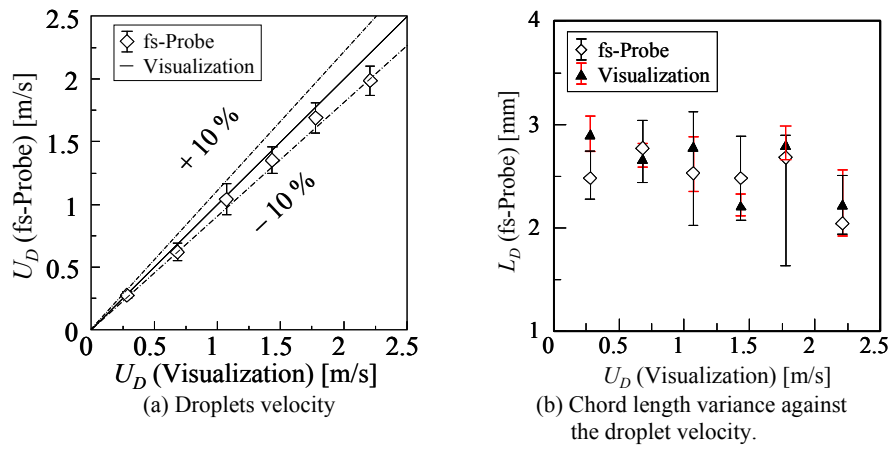


Figure 19. Comparison between ~~fs-Probe~~Es-TOP and visualization results (mm-size droplets).

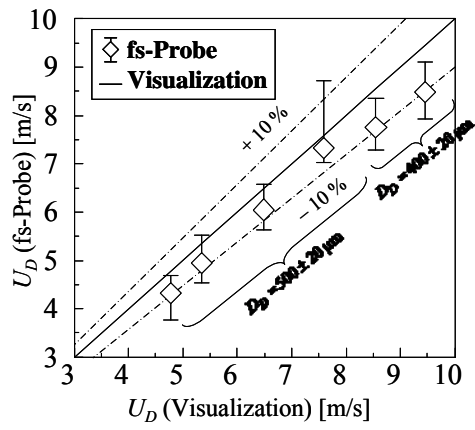
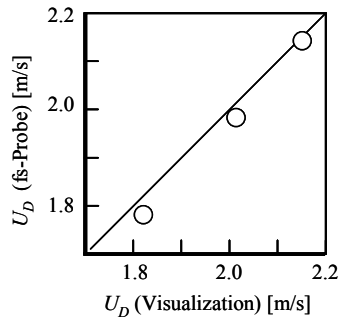


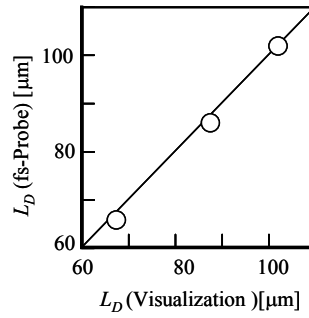
Figure 20. Comparison of fs-ProbeFs-TOP measurement results of sub-millimetre-size droplets between

Table 2. Differences of measurement results of sub-millimetre-size droplets between ~~fs-Probe~~ **Fs-TOP** and visualization

Visualization [m/s]	Fs-TOP [m/s]	Differences [%]
4.77	4.32	-9.5
5.35	4.95	-7.5
6.49	6.05	-6.8
7.59	7.33	-3.5
8.55	7.76	-9.2
9.46	8.49	-10.3



(a) Droplet velocities.



(b) Droplet chord lengths.

Figure 21. Comparison of fs-Probe measurement results of μ m-size droplets between fs-Probe and visualization results.

ページ - 3 -: [1] 書式変更 T. Saito 2009/06/26 23:43:00

フォント : Times New Roman

ページ - 3 -: [1] 書式変更 T. Saito 2009/06/26 23:43:00

フォント : Times New Roman

ページ - 3 -: [2] 書式変更 T. Saito 2009/06/26 23:43:00

フォント : Times New Roman

ページ - 3 -: [2] 書式変更 T. Saito 2009/06/26 23:43:00

フォント : Times New Roman

ページ - 3 -: [2] 書式変更 T. Saito 2009/06/26 23:43:00

フォント : Times New Roman

ページ - 3 -: [2] 書式変更 T. Saito 2009/06/26 23:43:00

フォント : Times New Roman

ページ - 3 -: [2] 書式変更 T. Saito 2009/06/26 23:43:00

フォント : Times New Roman

ページ - 3 -: [2] 書式変更 T. Saito 2009/06/26 23:43:00

フォント : Times New Roman

ページ - 3 -: [2] 書式変更 T. Saito 2009/06/26 23:43:00

フォント : Times New Roman

ページ - 3 -: [2] 書式変更 T. Saito 2009/06/26 23:43:00

フォント : Times New Roman

ページ - 3 -: [2] 書式変更 T. Saito 2009/06/26 23:43:00

フォント : Times New Roman

ページ - 3 -: [2] 書式変更 T. Saito 2009/06/26 23:43:00

フォント : Times New Roman

ページ - 3 -: [2] 書式変更 T. Saito 2009/06/26 23:43:00

フォント : Times New Roman

ページ - 3 -: [2] 書式変更 T. Saito 2009/06/26 23:43:00

フォント : Times New Roman

ページ - 3 -: [2] 書式変更 T. Saito 2009/06/26 23:43:00

フォント : Times New Roman

ページ - 3 -: [2] 書式変更 T. Saito 2009/06/26 23:43:00

フォント : Times New Roman

ページ - 3 -: [2] 書式変更 T. Saito 2009/06/26 23:43:00

フォント : Times New Roman

ページ - 3 -: [2] 書式変更 T. Saito 2009/06/26 23:43:00

フォント : Times New Roman

ページ - 3 -: [2] 書式変更 T. Saito 2009/06/26 23:43:00

フォント : Times New Roman

ページ - 3 -: [2] 書式変更 T. Saito 2009/06/26 23:43:00

フォント : Times New Roman

ページ - 3 -: [2] 書式変更 T. Saito 2009/06/26 23:43:00

フォント : Times New Roman

ページ - 3 -: [2] 書式変更 T. Saito 2009/06/26 23:43:00

フォント : Times New Roman

ページ - 3 -: [2] 書式変更	T. Saito	2009/06/26 23:43:00
---------------------	----------	---------------------

フォント : Times New Roman

ページ - 3 -: [2] 書式変更	T. Saito	2009/06/26 23:43:00
---------------------	----------	---------------------

フォント : Times New Roman

ページ - 3 -: [2] 書式変更	T. Saito	2009/06/26 23:43:00
---------------------	----------	---------------------

フォント : Times New Roman

ページ - 3 -: [2] 書式変更	T. Saito	2009/06/26 23:43:00
---------------------	----------	---------------------

フォント : Times New Roman

ページ - 3 -: [2] 書式変更	T. Saito	2009/06/26 23:43:00
---------------------	----------	---------------------

フォント : Times New Roman

ページ - 3 -: [2] 書式変更	T. Saito	2009/06/26 23:43:00
---------------------	----------	---------------------

フォント : Times New Roman

ページ - 3 -: [2] 書式変更	T. Saito	2009/06/26 23:43:00
---------------------	----------	---------------------

フォント : Times New Roman

ページ - 3 -: [2] 書式変更	T. Saito	2009/06/26 23:43:00
---------------------	----------	---------------------

フォント : Times New Roman

ページ - 3 -: [2] 書式変更	T. Saito	2009/06/26 23:43:00
---------------------	----------	---------------------

フォント : Times New Roman

ページ - 3 -: [2] 書式変更	T. Saito	2009/06/26 23:43:00
---------------------	----------	---------------------

フォント : Times New Roman

ページ - 3 -: [2] 書式変更	T. Saito	2009/06/26 23:43:00
---------------------	----------	---------------------

フォント : Times New Roman

ページ - 3 -: [2] 書式変更	T. Saito	2009/06/26 23:43:00
---------------------	----------	---------------------

フォント : Times New Roman

ページ - 3 -: [3] 書式変更	T. Saito	2009/11/05 11:54:00
---------------------	----------	---------------------

フォントの色 : 自動

ページ - 3 -: [3] 書式変更	T. Saito	2009/11/05 11:54:00
---------------------	----------	---------------------

フォントの色 : 自動

ページ - 3 -: [3] 書式変更	T. Saito	2009/11/05 11:54:00
---------------------	----------	---------------------

フォントの色 : 自動

ページ - 3 -: [3] 書式変更	T. Saito	2009/11/05 11:54:00
---------------------	----------	---------------------

フォントの色 : 自動

ページ - 3 -: [3] 書式変更	T. Saito	2009/11/05 11:54:00
---------------------	----------	---------------------

フォントの色 : 自動

ページ - 3 -: [3] 書式変更	T. Saito	2009/11/05 11:54:00
---------------------	----------	---------------------

フォントの色 : 自動

ページ - 3 -: [3] 書式変更	T. Saito	2009/11/05 11:54:00
---------------------	----------	---------------------

フォントの色 : 自動

ページ - 3 -: [3] 書式変更	T. Saito	2009/11/05 11:54:00
---------------------	----------	---------------------

フォントの色 : 自動

ページ - 3 -: [3] 書式変更	T. Saito	2009/11/05 11:54:00
---------------------	----------	---------------------

フォントの色 : 自動

ページ - 3 -: [3] 書式変更	T. Saito	2009/11/05 11:54:00
---------------------	----------	---------------------

フォントの色 : 自動

ページ - 3 -: [3] 書式変更 T.Saito 2009/11/05 11:54:00

フォントの色 : 自動

ページ - 3 -: [3] 書式変更 T.Saito 2009/11/05 11:54:00

フォントの色 : 自動

ページ - 3 -: [3] 書式変更 T.Saito 2009/11/05 11:54:00

フォントの色 : 自動

ページ - 3 -: [3] 書式変更 T.Saito 2009/11/05 11:54:00

フォントの色 : 自動

ページ - 3 -: [3] 書式変更 T.Saito 2009/11/05 11:54:00

フォントの色 : 自動

ページ - 3 -: [3] 書式変更 T.Saito 2009/11/05 11:54:00

フォントの色 : 自動

ページ - 3 -: [3] 書式変更 T.Saito 2009/11/05 11:54:00

フォントの色 : 自動

ページ - 3 -: [3] 書式変更 T.Saito 2009/11/05 11:54:00

フォントの色 : 自動

ページ - 3 -: [3] 書式変更 T.Saito 2009/11/05 11:54:00

フォントの色 : 自動

ページ - 3 -: [3] 書式変更 T.Saito 2009/11/05 11:54:00

フォントの色 : 自動

ページ - 3 -: [3] 書式変更 T.Saito 2009/11/05 11:54:00

フォントの色 : 自動

ページ - 3 -: [3] 書式変更	T.Saito	2009/11/05 11:54:00
---------------------	---------	---------------------

フォントの色 : 自動

ページ - 3 -: [3] 書式変更	T.Saito	2009/11/05 11:54:00
---------------------	---------	---------------------

フォントの色 : 自動

ページ - 3 -: [3] 書式変更	T.Saito	2009/11/05 11:54:00
---------------------	---------	---------------------

フォントの色 : 自動

ページ - 3 -: [3] 書式変更	T.Saito	2009/11/05 11:54:00
---------------------	---------	---------------------

フォントの色 : 自動

ページ - 3 -: [3] 書式変更	T.Saito	2009/11/05 11:54:00
---------------------	---------	---------------------

フォントの色 : 自動

ページ - 3 -: [3] 書式変更	T.Saito	2009/11/05 11:54:00
---------------------	---------	---------------------

フォントの色 : 自動

ページ - 3 -: [3] 書式変更	T.Saito	2009/11/05 11:54:00
---------------------	---------	---------------------

フォントの色 : 自動

ページ - 3 -: [3] 書式変更	T.Saito	2009/11/05 11:54:00
---------------------	---------	---------------------

フォントの色 : 自動

ページ - 3 -: [3] 書式変更	T.Saito	2009/11/05 11:54:00
---------------------	---------	---------------------

フォントの色 : 自動

ページ - 3 -: [3] 書式変更	T.Saito	2009/11/05 11:54:00
---------------------	---------	---------------------

フォントの色 : 自動